

The Geological Society Special Publications

Caledonian and pre-Caledonian orogenic events in Shetland, Scotland: evidence from garnet Lu-Hf and Sm-Nd geochronology --Manuscript Draft--

Manuscript Number:	GSLSpecPub2020-32R1
Article Type:	Research article
Full Title:	Caledonian and pre-Caledonian orogenic events in Shetland, Scotland: evidence from garnet Lu-Hf and Sm-Nd geochronology
Short Title:	Garnet Lu-Hf and Sm-Nd dating of metamorphism in Shetland
Corresponding Author:	Stephanie Walker Boston College Chestnut Hill, Massachusetts UNITED STATES
Corresponding Author E-Mail:	walkerfj@bc.edu
Other Authors:	Anna F. Bird Matthew F. Thirlwall Rob A. Strachan
Order of Authors (with Contributor Roles):	Stephanie Walker (Conceptualization: Equal; Data curation: Lead; Formal analysis: Lead; Investigation: Lead; Visualization: Lead; Writing – original draft: Lead; Writing – review & editing: Equal) Anna F. Bird (Conceptualization: Supporting; Investigation: Supporting; Methodology: Supporting; Supervision: Supporting; Writing – review & editing: Supporting) Matthew F. Thirlwall (Conceptualization: Equal; Data curation: Supporting; Formal analysis: Supporting; Methodology: Lead; Resources: Lead; Supervision: Lead; Writing – review & editing: Supporting) Rob A. Strachan (Conceptualization: Equal; Formal analysis: Supporting; Investigation: Supporting; Supervision: Supporting; Visualization: Supporting; Writing – review & editing: Supporting)
Abstract:	Garnet Lu-Hf and Sm-Nd ages from the Shetland Caledonides provide evidence of a polyorogenic history as follows: 1) c. 1050 Ma Grenvillian reworking of Neoproterozoic basement; 2) c. 910 Ma Renlandian metamorphism of the Westing Group; 3) c. 622-606 Ma metamorphism of the Walls Metamorphic Series but of uncertain significance because the eastern margin of Laurentia is thought to have been in extension at that time; 4) Grampian I ophiolite obduction at c. 491 Ma followed by crustal thickening and metamorphism between c. 485 and c. 466 Ma; 5) Grampian II metamorphism between c. 458 and c. 442 Ma that appears to have been focused in areas where pre-existing foliations were gently-inclined and thus may have been relatively easily reworked; 6) Scandian metamorphism at c. 430 Ma, although the paucity of these ages suggests that much of Shetland did not attain temperatures for garnet growth. There is no significant difference in the timing of Caledonian orogenic events either side of the Walls Boundary Fault, although this need not preclude linkage with the Great Glen Fault. However, the incompatibility of Ediacaran events either side of the Walls Boundary Fault may indicate significant lateral displacement and requires further investigation.
Section/Category:	Pannotia to Pangaea: Neoproterozoic and Paleozoic Orogenic Cycles in the Circum-Atlantic Region
Additional Information:	
Question	Response
Are there any conflicting interests, financial or otherwise?	No
Samples used for data or illustrations in	Confirmed

this article have been collected in a responsible manner

1 Caledonian and pre-Caledonian orogenic events in Shetland, Scotland: evidence
2 from garnet Lu-Hf and Sm-Nd geochronology

3

4 S. Walker^{1,2}, A.F. Bird^{1,3}, M.F. Thirlwall¹, R.A. Strachan⁴

5

6 1. Department of Earth Sciences, Royal Holloway University of London, London, TW20 0EX, UK

7 2. Center for Isotope Geochemistry, Boston College, Chestnut Hill, Massachusetts, 02467, USA.

8 3. Department of Geography, Geology, and Environment, University of Hull, Hull, HU6 7RX, UK

9 4. School of the Environment, Geography and Geosciences, University of Portsmouth, Portsmouth, PO1
10 3QL, UK.

11

12

13 **Abstract**

14 Garnet Lu-Hf and Sm-Nd ages from the Shetland Caledonides provide evidence of a polyorogenic
15 history as follows: 1) c. 1050 Ma Grenvillian reworking of Neoproterozoic basement; 2) c. 910 Ma
16 Renlandian metamorphism of the Westing Group; 3) c. 622-606 Ma metamorphism of the Walls
17 Metamorphic Series but of uncertain significance because the eastern margin of Laurentia is
18 thought to have been in extension at that time; 4) Grampian I ophiolite obduction at c. 491 Ma
19 followed by crustal thickening and metamorphism between c. 485 and c. 466 Ma; 5) Grampian II
20 metamorphism between c. 458 and c. 442 Ma that appears to have been focused in areas where
21 pre-existing foliations were gently-inclined and thus may have been relatively easily reworked;
22 6) Scandian metamorphism at c. 430 Ma, although the paucity of these ages suggests that much
23 of Shetland did not attain temperatures for garnet growth. There is no significant difference in
24 the timing of Caledonian orogenic events either side of the Walls Boundary Fault, although this
25 need not preclude linkage with the Great Glen Fault. However, the incompatibility of Ediacaran
26 events either side of the Walls Boundary Fault may indicate significant lateral displacement and
27 requires further investigation.

28

29

30

[end of abstract]

31 The pre-Devonian rocks of Shetland (northern Scotland) form part of the North Atlantic
32 Caledonides, which resulted from the Ordovician-Devonian closure of the Iapetus Ocean and
33 collision of Laurentia, Baltica and Avalonia. Rocks affected by the Caledonian orogeny currently
34 crop out in the North Atlantic region in the British Isles, Ireland, Greenland and Scandinavia (Fig.
35 1A). In mainland Scotland (Laurentia), the Caledonian orogeny resulted from two Ordovician
36 accretionary events and the culminating Siluro-Devonian continental collision (Lambert &
37 McKerrow 1976; Oliver et al. 2000; Chew et al. 2010; Bird et al. 2013; Tanner 2014; Dewey et al.
38 2015). The rock units affected by these orogenic events in the high-grade 'orthotectonic' zone
39 north of the Highland Boundary Fault-Clew Bay Line (Fig. 1A) were deposited between the early
40 Neoproterozoic and the Cambrian. The distinction between geological structures and
41 metamorphic assemblages formed in the various Ordovician-Silurian orogenic events in this
42 sector of the Caledonides therefore relies almost entirely on geochronological studies and is
43 commonly problematic.

44 Shetland is the northernmost sector of the Scottish Caledonides, situated almost
45 equidistant between mainland Scotland, and the western Scandinavian Caledonides in Norway
46 (Baltica) (Fig. 1A). Despite the importance of Shetland as a central location between the Scottish
47 and Scandinavian Caledonides, relatively few modern geochronological studies have been
48 undertaken here. Most recent published geochronological studies of the timing of
49 metamorphism in Shetland have utilized the U-Pb system in monazite and zircon (Cutts et al.
50 2009, 2011; Crowley & Strachan 2015; Jahn et al. 2017). These systems are extremely robust
51 against alteration and retrogression, and high-spatial resolution methods (e.g. LA-ICPMS or SIMS)
52 allow for targeting specific regions within an individual crystal. However, that zircons are so
53 robust can be problematic when utilized to understand low- and medium-grade metamorphic
54 rocks, as they may have been inherited (as a detrital mineral or from an igneous protolith), and
55 do not commonly crystallize at these temperatures and pressures (see however Dempster et al.
56 2004). For monazite U-Pb this is less of an issue as it can crystallize at lower temperatures and
57 pressures. A further limitation is that it can be difficult to relate accessory minerals such as zircon
58 and monazite to specific deformation fabrics and metamorphic assemblages. In contrast, here
59 we utilize Lu-Hf and Sm-Nd geochronology to establish the timing of garnet growth in Shetland.

60 This approach has three key advantages: 1) garnet is a common metamorphic mineral that
61 crystallizes over a wide range of pressures and temperatures, 2) garnet often forms
62 porphyroblasts that can be related to deformation fabrics and therefore provide age constraints
63 on tectonic structures, and 3) garnet can be dated accurately and precisely using two different
64 isotopic systems (Lu-Hf and Sm-Nd).

65 This study aims to test existing models for the timing of Caledonian and pre-Caledonian
66 metamorphic episodes in Shetland using Lu-Hf and Sm-Nd garnet geochronology, and thus
67 provide key correlations with related areas elsewhere in the orogen.

68

69 **Geological setting**

70 ***Tectonic overview of the Scottish Caledonides***

71 In Scotland and Ireland, Caledonian convergent tectonics began during the late Cambrian to early
72 Ordovician (c. 480-470 Ma) when the Laurentian margin collided with an intra-oceanic arc that
73 had developed above an oceanward-dipping subduction zone (Dewey & Ryan 1990). Supra-
74 subduction zone ophiolites were obducted onto the Laurentian margin (Dewey & Shackleton
75 1984; Chew et al 2010), and crop out along the Highland Boundary Fault – Fair Head-Clew Bay
76 Line (Fig. 1A.). The best exposed of these is the Shetland Ophiolite Complex, which crops out on
77 the islands of Unst and Fetlar in northern Shetland (Fig. 1B; Garson & Plant 1973; Flinn 1985;
78 Prichard 1985). The early-to-mid Ordovician arc-continent collision resulted in the Grampian
79 orogeny and widespread regional deformation and Barrovian metamorphism of the Moine and
80 Dalradian supergroups that are exposed, respectively in the Northern Highland and Grampian
81 terranes (Fig 1A; Lambert & McKerrow 1976; Oliver et al. 2000; Chew et al. 2010; Bird et al. 2013;
82 Tanner 2014). Arc-continent collision was followed by a reversal of subduction polarity and
83 development of an accretionary prism in the Southern Uplands Terrane (Leggett et al. 1979).

84 A late Ordovician metamorphic event, termed 'Grampian II' resulted in widespread
85 garnet growth at c. 450-445 Ma in the western part of the Moine Supergroup (Bird et al. 2013)
86 and mica fabrics also formed at this time in Shetland (Walker et al. 2016). However, whether this
87 event was caused by the collision of a micro-continental fragment with the margin of Laurentia
88 (Bird et al. 2013) or flat-slab subduction (Dewey et al. 2015) is uncertain.

89 Sinistrally oblique collision of Baltica and Laurentia occurred in the Silurian-Devonian
90 during the Scandian event (Gee 1975; Soper et al. 1992; Dewey & Strachan 2003). In Scotland,
91 this event only caused significant deformation and metamorphism in the Northern Highland
92 Terrane, which was opposite southern Baltica during continental collision (Coward 1990;
93 Dallmeyer et al. 2001; Dewey & Strachan 2003). Late-orogenic sinistral displacement of c. 700-
94 500 km along the Great Glen Fault juxtaposed the Northern Highland and Grampian terranes of
95 mainland Scotland (Dewey & Strachan 2003). Late- to post-orogenic extensional and
96 transtensional faulting formed the basins in which the Siluro-Devonian 'Old Red Sandstone'
97 clastic sediments were deposited (Seranne 1992; Dewey & Strachan 2003; Wilson et al. 2010;
98 Dichiarante et al. 2016).

99 There is widespread evidence for Neoproterozoic orogenic events in the Northern
100 Highland and Grampian terranes of mainland Scotland and Shetland, despite extensive
101 Caledonian re-working. Isotopic ages obtained from metamorphic assemblages and syn-tectonic
102 pegmatites cluster at 940-930 Ma ('Renlandian'), 820-780 Ma and 740-725 Ma ('Knoydartian')
103 and are interpreted to date pulses of prograde amphibolite facies metamorphism (Noble et al.
104 1996; Rogers et al. 1998; Vance et al. 1998; Highton et al. 1999; Tanner & Evans 2003; Cutts et
105 al. 2009, 2010; Cawood et al. 2015; Jahn et al. 2017; Bird et al. 2018). During the Neoproterozoic,
106 Scotland was likely located close to the edge of Rodinia and these and potentially correlative
107 metamorphic events in eastern Laurentian rocks of East Greenland, Svalbard and Pearya have
108 been interpreted as resulting from periods of accretionary orogenesis in the hangingwall of a
109 continentward-dipping subduction zone (Cawood et al., 2010; Malone et al., 2017).

110

111 ***Caledonian geology of Shetland***

112 The c. N-S trending Walls Boundary Fault (WBF) in Shetland (Fig. 1B) has been interpreted as the
113 northern continuation of the Great Glen Fault (Flinn 1961, 1977, 1992; Watts et al. 2007) and
114 provides a convenient basis for subdividing the pre-Devonian geology. If correct, this linkage
115 implies that the rocks to the west of the WBF form part of the Northern Highland Terrane, and
116 the rocks to the east part of the Grampian Terrane. However, the magnitude of displacements
117 along, and potential correlations across this fault are uncertain.

118 *West of the Walls Boundary Fault*

119 Late Caledonian igneous rocks and Devonian sediments dominate the geology to the west of the
120 Walls Boundary Fault (Fig. 1B). Greenschist to amphibolite facies metamorphic units crop out at
121 North Roe, Hillswick, and on the north coast of the Walls Peninsula (Fig. 1B).

122 In northwestern Shetland, the east-dipping Wester Keolka Shear Zone (WKSZ) separates
123 the Archaean Uyea Gneiss Complex (Kinny et al. 2019) from the Sand Voe Group (SVG)
124 metasediments (Pringle 1970). This structure has been regarded as an extension of the Moine
125 Thrust Zone which defines the northwest margin of the Caledonides in mainland Scotland (Fig.
126 1A; Andrews 1985; Ritchie et al 1987; Flinn 1992; 1993; McBride & England 1994). However, the
127 lowermost part of the SVG contains pebbles that are lithologically similar to the underlying Uyea
128 Gneiss Complex (Pringle 1970, Kinny et al 2019), indicating that the WKSZ may in fact be a
129 tectonically modified unconformity. Further, the penetrative mica fabric in the WKSZ has been
130 dated as Neoproterozoic using Rb-Sr mica geochronology (Walker et al. 2016). Both lines of
131 evidence suggest that the WKSZ is not the equivalent of the Moine Thrust. The Devonian Uyea
132 Shear Zone c. 2 km to the west may be structurally equivalent to the Moine Thrust or any
133 correlative may be located offshore (Walker et al. 2016). The Sand Voe Group psammities have
134 been correlated on lithological grounds with the Moine Supergroup in mainland Scotland (Flinn
135 1988). Farther east, the SVG is overthrust by felsic and mafic orthogneisses, the 'Eastern
136 Gneisses', which have been regarded as equivalent to the Archaean basement inliers found
137 within the Northern Highland Terrane in mainland Scotland (Flinn 1988). The Virdibreck Shear
138 Zone separates these from the Queyfirth Group, a series of metasediments and metavolcanics
139 which may correlate with the Dalradian Supergroup in mainland Scotland (Flinn et al. 1972; Flinn
140 2007).

141 The Hillswick area (Fig. 1B) contains units that have been correlated with the Eastern
142 Gneisses, the Sand Voe Group, and the Queyfirth Group. On the northern margin of Walls
143 Peninsula (Fig. 1B), the Walls Metamorphic Series comprises quartzofeldspathic gneisses,
144 amphibolites, limestones, and calc-silicates. The foliation strikes east-west and dips gently
145 southwards. Whilst being distinct from other lithologies in Shetland (Flinn et al. 1979), Mykura
146 (1976) proposed a similar tectonic and amphibolite to greenschist facies metamorphic history to

147 the Sand Voe Group. Hornblende K-Ar ages ranging from c. 863-363 Ma have been interpreted
148 as indicating that the earliest prograde metamorphism of the Walls Metamorphic Series occurred
149 during the Grenvillian orogeny (Flinn et al. 1979). However, Rb-Sr white mica ages (Walker et al.
150 2016) indicate fabric development at c. 500 Ma and c. 450 Ma, suggesting a multiphase
151 Caledonian history with no evidence for an older Grenvillian component.

152 *East of the Walls Boundary Fault*

153 The geology east of the WBF is dominated by two major metasedimentary successions: the Yell
154 Sound Group (YSG) and the East Mainland Succession (EMS) (Fig. 1B). Regional foliation trends
155 N-S and dips steeply, except on Unst where it dips gently to moderately east. The YSG is the older
156 of the two and is exposed on Mainland Shetland and on Yell. The dominant lithologies are
157 psammitic and semi-pelitic gneisses with subordinate quartzites (Flinn 1988). The succession has
158 a structural thickness of 10 km (Flinn 1988), but in the absence of any sedimentary structures it
159 is difficult to know how closely this approximates to original depositional thickness. Flinn (1988)
160 correlated the YSG with the Moine Supergroup in mainland Scotland. The YSG metasediments
161 are intruded by pre- to syn-tectonic felsic orthogneisses and mafic amphibolites (Flinn 1994), and
162 are interleaved with Meso-Neoproterozoic TTG orthogneisses, similar to the Lewisian basement
163 gneisses of northwest mainland Scotland (Jahn et al. 2017). In NE Yell, one of these basement
164 inliers separates the YSG from the much thinner and lithologically contrasting Westing Group,
165 also found in west Unst (Fig. 1B). This comprises marbles and pelites and may form part of the
166 same sedimentary package as the Yell Sound Group.

167 Overlying the Westing Group on Unst, and the YSG on Mainland Shetland, the eastward-
168 younging East Mainland Succession (EMS) comprises psammities, pelites, marbles, and meta-
169 volcanics that are lithologically similar to the Dalradian Supergroup in mainland Scotland (Flinn
170 et al. 1972; Flinn 2007). However, differences in the timing of deposition and thickness of the
171 succession suggest that the EMS may have been deposited in a separate basin (Strachan et al.
172 2013). Metamorphic grade is highest in the western and lowest parts of the succession which
173 contain kyanite, staurolite, and garnet, progressively decreasing eastwards to upper greenschist
174 facies assemblages (Flinn et al. 2013).

175 On Unst and Fetlar (Fig. 1B), the East Mainland Succession is structurally overlain by the
176 Shetland Ophiolite Complex (Flinn 1958). This is disposed in two thrust sheets, and comprises
177 serpentinitised meta-harzburgite and metadunite, metaclinopyroxenite, and metagabbro, all
178 metamorphosed to greenschist facies (Flinn 1985; Prichard 1985). Chemical characteristics of
179 these units indicate formation in a supra-subduction zone setting (Spray & Dunning 1991;
180 Prichard et al 1996; Flinn 2001; O'Driscoll et al 2012). In contrast, the tectonic slices of a
181 metamorphic sole that underlie the ophiolite on Unst and Fetlar have MORB-type chemistry and
182 record upper amphibolite facies metamorphism (Spray 1988). These are interpreted as remnants
183 of subducted oceanic lithosphere that were juxtaposed against the ophiolite during its obduction
184 (Spray 1988). The lower ophiolite sheet is overlain by the metasedimentary rocks of the Muness
185 Phyllite, and, on Fetlar, the deformed and metamorphosed Funzie Conglomerate (Flinn 2014).

186 *Structural and metamorphic framework*

187 Published data indicate the following sequence of Proterozoic and Caledonian events in Shetland:

- 188 1) The Yell Sound and Westing groups were deposited after c. 1020 Ma (the age of the
189 youngest detrital zircons that they contain (Cutts *et al* 2009)) and affected by high-grade
190 Renlandian metamorphism at 940-920 Ma (U-Pb zircon and monazite; Cutts et al. 2009,
191 2011; Jahn et al. 2017).
- 192 2) Deposition of the East Mainland Succession is believed to have been initiated after c. 700
193 Ma as a result of the breakup of Pannotia which culminated in the formation of the
194 Iapetus Ocean (Prave et al. 2009).
- 195 3) 'Grampian I' regional deformation (D1) and amphibolite facies metamorphism of the Yell
196 Sound and Westing groups and the East Mainland Succession is thought to have occurred
197 at c. 485-475 Ma and to have resulted from crustal thickening that accompanied and
198 followed ophiolite obduction (Fig. 2; Cutts et al. 2011). The ophiolite is known to have
199 formed at 492 ± 3 Ma, the U-Pb zircon age of a plagiogranite (Spray & Dunning 1991), and
200 was obducted at 484 ± 4 Ma, as constrained by a U-Pb zircon age from the metamorphic
201 sole (Crowley & Strachan 2015). The transport direction is believed to have been towards
202 the west, based on kinematic and lineation data preserved in west Unst (Cannat 1989;

203 Flinn & Oglethorpe 2005; Flinn 2014). Peak pressure-temperature conditions were c. 10
204 kbar and c. 775°C (Cutts et al. 2011).

205 4) Reworking of thrust-related fabrics into a regionally steep (D2) orientation across Yell and
206 much of Mainland Shetland was likely complete by c. 465-460 Ma (Walker et al. 2016)
207 and certainly by 464.6 ± 4.6 Ma, the age of the late- to post-tectonic Brae Pluton (Fig. 1B;
208 U-Pb zircon; Lancaster et al. 2017). When traced eastwards, the composite D1/D2
209 foliation progressively shallows to dip west to define the lower limb of a large-scale,
210 eastward-closing recumbent fold (Fig. 2; the 'Shetland Mega-Monocline' of Flinn 2007).
211 The precise mechanism for formation of this fold is uncertain, but it may have developed
212 at a late stage during D2.

213 5) 'Grampian II' metamorphism of metasedimentary successions at c. 450-445 Ma (Rb-Sr
214 muscovite; Walker et al. 2016), although little is understood of the tectonic driver of this
215 event. It could have resulted from accretion of an arc or microcontinental fragment to the
216 Laurentian margin (Bird et al. 2013) or flat-slab subduction (Dewey et al. 2015).

217 6) Sinistrally-oblique, top-to-the-NNE shear on Unst and Fetlar juxtaposed the lower
218 ophiolite thrust sheets against their current footwall rocks (Cannat 1989; Beijat et al.
219 2018). The associated deformation fabrics are recorded in the Funzie Conglomerate and
220 so must be younger than its depositional age, i.e. <440 Ma (Beijat et al. 2018). This is
221 consistent with Rb-Sr mica ages of c. 440-430 Ma obtained in west Unst and also thought
222 to date this deformation event (Walker et al. 2016). The tectonic driver is unknown: did
223 it result from gravitational instability arising from crustal thickening at a deeper structural
224 level, or from sinistral relative displacement between Laurentia and Baltica following
225 oblique continental collision (Dewey & Strachan 2003)?

226 7) Scandian (c. 430-410 Ma) westerly-directed thrusting is indicated by emplacement of the
227 upper ophiolite nappe onto the Funzie Conglomerate on Fetlar (Beijat et al. 2018) and
228 displacement on the Uyea Shear Zone (Walker et al. 2016). The upper ophiolite nappe is
229 believed to be the same tectonic unit as the lower ophiolite nappe, repeated by thrusting.

230

231 **Sample descriptions**

232 Twenty-two samples were collected to provide geochronological insights into the timing of
233 garnet growth and metamorphism in the Caledonian rocks of Shetland. Key targets for sample
234 collection were metamorphic lithologies to the west of the Walls Boundary Fault, where there
235 are relatively few modern geochronological constraints. Sample numbers, location, lithologies,
236 structural significance, and metamorphic assemblages can be found in Table 1.

237

238 **Analytical methods**

239 Samples were crushed in a steel jaw-crusher to chips of $< 1\text{cm}^3$. A fraction of this crushed material
240 was saved for whole rock analysis, which was powdered in a tungsten carbide TEMA mill ready
241 for XRF and isotopic analysis. This remaining material was sieved to different grain sizes, washed
242 repeatedly in de-ionised water, and magnetically separated using a Frantz isodynamic separator.
243 Garnets and other mineral fractions were handpicked under a binocular microscope from the
244 250-500 μm magnetic fraction, taking care to pick only grains that were visibly inclusion-free.
245 Some samples had multiple populations of garnets, recognised by different colours, and assumed
246 to represent different garnet age-populations. This assumption of the relationship between
247 colour and garnet population was supported by close inspection of hand-specimen, petrographic
248 thin-section, and both colour and chemistry of the crystals analysed by LA-ICPMS (Fig. 3). Where
249 multiple garnet fractions of a sample are noted, each individual fraction represents a new
250 separation from the picking stage of preparation.

251 Prior to isotopic analysis, representative garnet crystals from each sample were analysed
252 for trace element, and selected major element, concentrations using the LA-ICPMS system at
253 RHUL (methods outlined in Müller et al. 2009 and Bird et al. 2013). Traverses were the preferred
254 method of data acquisition as they permit detailed study of garnet zoning profiles and tentative
255 identification of mineral inclusions. Laser ablation spot size, laser repetition rates, and scan speed
256 were 15 μm , 10 Hz, and 0.6 mm s^{-1} respectively, and data were calibrated against the NIST612
257 standard glass.

258 Amounts of mixed ^{176}Lu - ^{180}Hf and ^{149}Sm - ^{150}Nd spikes for mineral separates and whole-
259 rocks were estimated using concentrations of these elements, and of analogues such as Y and Zr,
260 from LA-ICPMS and XRF respectively. Leaching, spiking, dissolution, and chemical separation

261 procedures were those of Anczkiewicz & Thirlwall (2003), and Bird et al. (2013), with
262 concentrations and isotopic data being determined on the same aliquot. A HF-HNO₃ digestion
263 procedure was utilized for garnets in sealed beakers on a hotplate, followed by a dissolution
264 check in 6M HCl. This should minimize dissolution of refractory zircon inclusions, which can
265 worsen the precision of Lu-Hf ages, as they have very high Hf concentrations. Further, detrital
266 zircons in metasediments can be much older than the surrounding garnets, which may artificially
267 skew the age of any mixtures of garnets and zircons (Anczkiewicz et al. 2004). A moderate
268 leaching procedure using sulfuric acid was performed on all garnet fractions, after the methods
269 of Anczkiewicz & Thirlwall (2003), attempting to dissolve phosphate inclusions that can
270 negatively affect Sm-Nd ages. A more rigorous leaching procedure, such as that of Baxter et al
271 (2002) using HF, was not used because, while it is clear that this procedure is excellent for
272 producing 'clean' garnet fractions with high Sm/Nd ratios for Sm-Nd dating, no testing has been
273 done on this procedure for Lu-Hf dating, and may fractionate Lu from Hf.

274 For the whole-rock fractions analysed for Lu-Hf, we treated one fraction in the same
275 manner as the garnets (table-top dissolution using HF-HNO₃), and a second whole-rock powder
276 fraction was fused for one hour at 1100°C in Pt-Au crucibles in a 1:3 ratio with lithium tetraborate
277 flux. Glass fragments were then spiked and subjected to the normal Lu-Hf dissolution and
278 chemical separation. Blanks were 60pg Hf and 85pg Lu, which is insignificant based on the
279 amount of analyte for these elements.

280 Most Lu, Hf, and all Sm and Nd isotopic analyses were undertaken on the GV Instruments
281 IsoProbe MC-ICPMS at RHUL using methods outlined in Thirlwall & Anczkiewicz (2004), and Bird
282 et al (2013). One batch of samples (those marked with § in Table 2) was analysed on the Thermo
283 *Neptune* MC-ICPMS at the Institute of Geological Sciences (IGS), Polish Academy of Sciences,
284 Kraków Research Centre following a similar analytical procedure to that described in Thirlwall &
285 Anczkiewicz (2004).

286 During the course of the study the Hf standard JMC475 analysed on the RHUL IsoProbe
287 yielded an average (static) ¹⁷⁶Hf/¹⁷⁷Hf of 0.282182±12 and ¹⁸⁰Hf/¹⁷⁷Hf of 1.88683±17 (2sd, n=36),
288 with no significant change with time. The same standard analysed on the Neptune at IGS yielded
289 respective ¹⁷⁶Hf/¹⁷⁷Hf and ¹⁸⁰Hf/¹⁷⁷Hf ratios of 0.282158±08, and 1.88687±10 (2sd, n=8). All

290 sample data were corrected to the accepted JMC475 $^{176}\text{Hf}/^{177}\text{Hf}$ value of 0.282165 (Scherer et al.
291 2000).

292 In contrast to Hf, Nd standard isotope ratios can vary significantly between analytical
293 sessions (Thirlwall and Anczkiewicz 2004), although the effect of this on ages was minimized by
294 analyzing all fractions relating to a sample during one analytical session. The Aldrich Nd and
295 mixed Ce-Nd standard solutions yielded $^{142}\text{Nd}/^{144}\text{Nd}$ of 1.141461 ± 239 and a slope corrected (see
296 Thirlwall & Anczkiewicz 2004) $^{143}\text{Nd}/^{144}\text{Nd}$ of 0.511408 ± 14 (2sd, $n=97$). The uncertainty on the
297 $^{176}\text{Lu}/^{177}\text{Hf}$ ratio is less than 0.3% and assumed to be 0.3% in age calculations. The uncertainty on
298 the $^{147}\text{Sm}/^{144}\text{Nd}$ is less than 0.1% and assumed to be 0.1% in age calculations.

299 Isochron ages and uncertainties were calculated using IsoplotR (Vermeesch, 2018), using
300 the decay constants of $1.865 \times 10^{-11} \text{ a}^{-1}$ for ^{176}Lu (Scherer et al. 2001) and $6.54 \times 10^{-12} \text{ a}^{-1}$ for ^{147}Sm
301 (Lugmair & Marti 1978). All isotope data and age uncertainties are quoted at the 2-sigma level.

302 **Interpreting garnet ages**

303 When a garnet grows on the prograde path, the heavy rare earth elements (HREE), including Lu,
304 will partition into the garnet and produce a zoning profile with a large central peak, decreasing
305 exponentially in concentration towards the rim as the garnet rapidly depletes the surrounding
306 volume of HREE (Skora et al. 2006). However, this can be complicated if a garnet has experienced
307 metamorphic conditions above the temperature of diffusion, or has been subject to multiple
308 orogenic cycles. In these scenarios, the garnet Lu profile may be flattened and/or disrupted. It is
309 therefore important to assess the trace element zoning of a garnet before linking any determined
310 ages to a specific prograde event. Trace element traverses for representative garnet crystals from
311 most samples are provided in the supplementary information.

312 Studies that present Lu-Hf and Sm-Nd ages from the same garnet dissolution have
313 concluded that the Lu-Hf system has a higher closure temperature than Sm-Nd, due to
314 systematically older ages in the former (Scherer et al. 2000; Lapen et al. 2003; Skora et al. 2006;
315 Bird et al. 2013; Smit et al. 2013). It has been alternatively suggested that, rather than different
316 closure temperatures of the two systems, the difference lies in fundamentally different processes
317 recorded in the systems during garnet growth (Lapen et al. 2003; Bloch & Ganguly 2015). High
318 central Lu peaks, and relatively homogenous Sm profiles of garnets may skew ages towards

319 recording early and 'average' states of garnet growth respectively (Lapen et al. 2003; Skora et al.
320 2006), hence explaining the systematic differences in Sm-Nd and Lu-Hf ages for a given sample.
321 Alternatively, Bloch & Ganguly (2015) argue that the chemical differences between Lu^{3+} and Hf^{4+}
322 lead to preferential retention of radiogenic ^{176}Hf if metamorphic temperatures are above that of
323 diffusion for prolonged periods. This would produce anti-clockwise rotation of an isochron,
324 leading to erroneously old ages. They however point out that it is unlikely that natural garnets
325 would be affected significantly by this process providing they are greater than 0.5mm in diameter
326 and have not been subjected to temperatures exceeding 700°C for "unusually long periods".

327 In addition to potential differences in closure temperature for the Sm-Nd and Lu-Hf
328 systems in garnets, they both may be detrimentally affected by different mineral inclusions.
329 Zircons have the potential to seriously affect any Lu-Hf ages, especially if the zircons formed from
330 a reservoir that is considerably older than the timing of garnet formation. Very low Lu/Hf (as a
331 function of high Hf concentration) in zircons may have the effect of flattening the isochron,
332 leading to erroneously young ages, if the whole-rock analysis did not incorporate a similar zircon
333 population, for example if not all zircons in the whole rock powder were dissolved. Similarly, the
334 Sm-Nd system may be affected by light rare earth element (LREE)-rich inclusions such as apatite,
335 monazite, and epidote. The effect of these inclusions on a garnet Sm-Nd age could be similar to
336 that of zircon inclusions on the Lu-Hf system, as the LREE-rich inclusions would have significantly
337 higher concentration of the daughter element compared to the garnet (Anczkiewicz & Thirlwall
338 2003). Phosphate inclusions with high LREE can, in theory, be removed by sulphuric acid leaching,
339 as we did in this study (Anczkeiwicz & Thirlwall 2003). However, epidote inclusions are robust
340 against such procedures and can detrimentally affect Sm-Nd ages.

341

342 **Results**

343 The potential significance of a Lu-Hf or Sm-Nd garnet age will depend on the temperature and
344 duration of metamorphism, and the size and composition of the garnet (Baxter & Scherer 2013).
345 Providing a garnet grows below the closure temperature of the isotopic system (c. 650°C for Sm-
346 Nd, Baxter et al. 2017), then the age will most likely relate to the prograde history of the sample
347 (Ganguly & Tirone 1999, Baxter & Scherer 2013, Smit et al. 2013). The garnet ages for each

348 sample have been assessed with regards to petrological, chemical, and structural information
349 before assigning geological significance. The results and the new Lu-Hf and Sm-Nd garnet ages
350 are presented in Table 2, and are placed in their geological and geographical contexts in Fig. 4.

351

352 ***Hf concentrations in whole-rock (WR) samples***

353 Table 2 reports Lu, Hf, Sm and Nd concentrations in the analysed samples, which provide strong
354 constraints on what minerals have been digested. Measured Nd contents in WR samples (all
355 digested without flux-fusion on a hotplate, denoted as tt = tabletop) are similar to XRF Nd data
356 for the same samples (Supplementary data 1). The same tt WR powder fractions however yield
357 Hf contents that are much less than would be expected from XRF Zr/40, leading to $^{176}\text{Lu}/^{177}\text{Hf}$
358 ratios often > 0.2 , sometimes higher than $^{176}\text{Lu}/^{177}\text{Hf}$ measured on garnets from the same sample
359 (e.g. AB08-08). Hf contents in WR fractions digested after flux-fusion are however much higher,
360 1.8-50x higher than those measured on tt WR fractions, and similar to those expected from XRF
361 Zr/40. This implies that very little of the zircon content of WR samples was dissolved when no
362 flux-fusion took place, and that all or nearly all the zircon content was digested by flux fusion.
363 Notably, for more than half the samples, Hf contents of some or all of the garnet fractions are
364 significantly higher than the Hf contents of the tt WR fractions. Given that LA-ICP-MS data
365 (Supplementary data 2) show that Hf contents of pure garnets are usually 0.1-0.5ppm, the
366 identical tt digestion process must be dissolving a much greater proportion of the zircon
367 inclusions in garnet than it is dissolving zircons in the WR powder. This implies that ages
368 calculated from garnet and ttWR are likely to be in error. This is because the analysed garnets
369 include a zircon population, with potentially old unradiogenic Hf, that is not represented in the
370 ttWR analysis, and also because the $^{176}\text{Lu}/^{177}\text{Hf}$ ratios measured in the ttWR may have been
371 influenced by preferential leaching of Lu rather than Hf from partially dissolved zircon. In general
372 in this study, the ttWR does not lie on an isochron with garnet and flux-fused WR. Where the
373 garnet is radiogenic, the difference between ttWR and flux-fused WR has no significant effect on
374 the Lu-Hf age. Where the garnet has only moderate $^{176}\text{Lu}/^{177}\text{Hf}$, between 0.1 and 0.5, the choice
375 between tt and flux-fused WR often has a very large effect on age. Based on the preceding

376 discussion, the flux-fused WR is preferred, and this is supported by better MSWDs and more
377 plausible ages.

378

379 ***Walls Peninsula ages***

380 All three samples studied from the Walls Metamorphic Series (WMS: SW15-01, pelite; SW15-03,
381 granite gneiss; and SW15-06, amphibolite) yield some pre-Caledonian ages. All contain chlorite-
382 biotite assemblages suggesting metamorphic grades no higher than middle amphibolite facies.
383 Both garnet fractions in SW15-06 yield 606-622 Ma Lu-Hf ages and early to mid Ordovician Sm-
384 Nd ages of 483.3 ± 4.9 and 461.9 ± 3.7 Ma in the pink (core) and orange (rim) fractions
385 respectively. The garnets only have moderate $^{176}\text{Lu}/^{177}\text{Hf}$ (0.28-0.52), but both WR fractions lie
386 on isochrons with each individual garnet, suggesting that zircon inclusions have no significant
387 effect on the age. The orange garnet core of SW15-03 has very low $^{176}\text{Lu}/^{177}\text{Hf}$ (0.078) but
388 moderate $^{147}\text{Sm}/^{144}\text{Nd}$, and yields a suspect 689 ± 8 Ma Lu-Hf age but a 617 ± 9 Sm-Nd age
389 consistent with the Lu-Hf ages of SW15-06. The rims of this garnet yield early Ordovician ages by
390 both Lu-Hf (486.3 ± 2.5 Ma) and Sm-Nd (473.2 ± 6.2 Ma). Thirdly, the two garnet fractions of
391 SW15-01 yield Cambrian Lu-Hf ages of c. 510 Ma that are within error of each other, but no Sm-
392 Nd data were obtained for this sample. Sample SW13-17, collected just 4km away in the WMS,
393 yields a 510.0 ± 2.3 Ma white mica age (Walker et al., 2016, recalculated), within error of these
394 Lu-Hf ages.

395 There seems to be clear evidence for Ediacaran and Cambrian metamorphic events in the
396 Walls Peninsula. In SW15-03, the orange cores give older ages than the rims for both Lu-Hf and
397 Sm-Nd, with the Sm-Nd age younger in both core and rim. This can reasonably be explained by
398 two stage growth of the garnets, with the slightly younger Sm-Nd rim age perhaps explained by
399 lower closure temperatures for Sm-Nd in garnets (e.g. Yakymchuck et al 2015). The younger Sm-
400 Nd ages in SW15-06 would require Ordovician loss of radiogenic Nd from the whole garnet
401 crystals, rather than just the rim. This behaviour of the Sm-Nd system may reflect the relatively
402 high metamorphic grade of these samples. The amphibolite shows a syn-tectonic relationship
403 with surrounding deformed felsic sheets, and both are intruded by undeformed felsic sheets. All
404 of the deformed material in this area shares a strong gneissose fabric that dips towards the SSE.

405 This fabric can be observed in thin section of these samples and wraps the garnets. This fabric
406 was dated further to the west in the Walls Metamorphic Series, using white mica Rb-Sr, as having
407 formed at 450.8 ± 1.4 Ma (Walker et al. 2016). This indicates that the garnet-growth was not
408 coeval with the main fabric development, and that the Walls Metamorphic Series was subject to
409 late stage foliation development which was not accompanied by significant garnet growth.

410

411 ***Northwest Shetland ages***

412 Ages have been obtained from seven samples in the area of North Roe and Hillswick, in a region
413 that has been subjected to west-directed thrust-stacking. Ages seem to become progressively
414 older going up through the tectonostratigraphy. In the west, amphibolite SW15-12 occurs within
415 strongly reworked Archaean orthogneisses in the footwall of the WKSZ at North Roe (Fig. 4), and
416 yields a Silurian Lu-Hf age of 426.9 ± 2.5 Ma. It should be noted that no flux-fused WR is available
417 for this sample. However, it is an amphibolite with only 61 ppm Zr, so expected WR Hf of c.
418 1.5ppm is not much greater than the measured ttWR Hf of 0.54ppm. Further, the garnet has
419 high $^{176}\text{Lu}/^{177}\text{Hf}$ so small changes in WR Hf systematics would have little impact on the age. The
420 garnets in this sample are skeletal, as shown in the LA-ICPMS traverse, with large inclusions of
421 amphibole, plagioclase, and epidote. Nevertheless, the Lu profile exhibits prograde zoning (Fig.
422 5), suggesting that the Lu-Hf garnet age determined on this sample relates to the timing of peak
423 metamorphism in this area, although it is possible that the garnets in this sample are
424 amalgamations of multiple smaller garnets which can be observed in Fig. 5.

425 Five samples have been studied from the Sand Voe Group and Eastern Gneisses, between
426 the WKSZ and the Virdibreck shear zone. No evidence was found of pre-Caledonian ages, despite
427 the Eastern Gneisses being thought to represent basement inliers (Pringle 1970). A sample of the
428 Benigarth Pelite (AB08-11) on the Fethaland peninsula in northwestern Mainland records a late
429 Ordovician Lu-Hf age of 446.5 ± 1.3 (n=3, MSWD: 0.17). The garnets did not yield $^{147}\text{Sm}/^{144}\text{Nd}$
430 significantly higher than the WR. The Benigarth Pelite is mapped as part of the 'Eastern Gneisses'
431 (Pringle 1970) but could equally well represent an infold or tectonic slice of the Sand Voe Group.
432 White mica and quartz define the main fabric in the matrix of this sample and this fabric wraps

433 the garnets, therefore the top-to-the-west shear band fabric in this area has to have been formed
434 during or after this 446 Ma episode of garnet growth.

435 Garnet from another Sand Voe Group pelite (AB08-13), collected a few kilometres to the
436 southeast, also gives a late Ordovician Lu-Hf age of 456.7 ± 2.2 Ma for the orange fraction, and a
437 Sm-Nd isochron age of 470 ± 6 Ma ($n=3$, MSWD: 1.7). The purple garnet fraction has very low
438 $^{176}\text{Lu}/^{177}\text{Hf}$ (0.056) and thus the 582 ± 9 Ma age is not considered robust. The $^{147}\text{Sm}/^{144}\text{Nd}$ ratio
439 for the orange fraction is lower than that of the whole-rock, which indicates that the leaching
440 procedure has not produced a 'clean' fraction. However, the point lies on the isochron which
441 suggests that the low Sm/Nd inclusions were in isotopic equilibrium with the garnet and the rest
442 of the rock. On the Hillswick peninsula, a Hillswick Group pelite (SW13-27, correlated with the
443 Sand Voe Group) yields an almost identical Lu-Hf garnet age to AB08-13, of 458.8 ± 2.3 Ma from
444 orange garnets which we interpret as the garnet cores, and 453.0 ± 2.3 Ma from a red population
445 which we interpret as garnet rims. The cores of the garnets from this sample are inclusion-rich,
446 with quartz, biotite, and ilmenite. The inclusion trails are slightly curved and are perpendicular to
447 the main fabric. The rims of the garnets are inclusion-poor. That the garnets from this sample
448 record two different Late Ordovician ages may indicate that there was more than one pulse of
449 metamorphism at this time, or that garnet growth was protracted. Again like AB08-13, the Sm-
450 Nd ages from SW13-27 are substantially older than the Lu-Hf ages (478 ± 14 Ma and 505 ± 21 Ma
451 from the core and rim respectively, similar to the 470 ± 6 Ma Sm-Nd age of AB08-13), but these
452 have poor precision due to the unradiogenic nature of the garnet separates, which may also lead
453 to poor accuracy.

454 A "basement" amphibolite (AB08-12) was collected from the Fethaland peninsula 250m
455 SE of Benigarth Pelite AB08-11, and provides a 33 Ma older Lu-Hf age of 479.6 ± 1.2 ($n=3$, MSWD:
456 1.4, using two separate garnet fractions and flux-fused WR, with amphibole lying significantly
457 above this line). None of the garnet fractions, nor amphibole, yielded a useful Sm-Nd age
458 presumably because inclusions were inadequately removed by leaching. A second amphibolite
459 within the Eastern Gneisses SW13-08, yields mid-Ordovician Lu-Hf ages of 466.3 ± 2.2 Ma and
460 459.7 ± 4.3 Ma on orange and red garnet fractions respectively. This was collected c. 130m SE of

461 AB08-13 pelite and like AB08-12, gives Lu-Hf ages >10 Ma older than the nearby pelite. 150m NE
462 of SW13-08, Walker et al. (2016) reported a white mica Rb-Sr age of 443.2 ± 1.3 Ma.

463 To the east of the Virdibreck shear zone, SW15-05 is a rare amphibolite from the Queyfirth
464 Group, and yields an early Ordovician Lu-Hf age of 474.1 ± 3.8 Ma. Garnets in this sample are
465 small and partially retrogressed to chlorite, however the Lu profile determined using LA-ICPMS
466 indicates that the age relates to prograde growth, and that there was no significant diffusion or
467 exchange of the HREE during retrogression. For this sample, we have used the whole-rock that
468 underwent simple table-top dissolution rather than the one that underwent the fused stage of
469 processing, because the slope between the two whole rocks was significantly steeper than the
470 one between the garnets and the whole-rocks, which may imply that there is a significantly older
471 population of refractory minerals in the fused whole-rock, which would artificially skew the age.

472

473 ***East Mainland ages***

474 Only two samples have been studied from Mainland east of the Walls Boundary Fault. A semi-
475 pelitic gneiss from the East Mainland Succession in central Mainland (SW12-07) provides an early
476 Ordovician Lu-Hf age of 479.0 ± 1.5 Ma, and a somewhat younger Sm-Nd age of 470.7 ± 1.0 Ma,
477 which complements the 473.6 ± 0.9 Ma Rb-Sr white-mica age determined on this sample by
478 Walker et al. (2016). This suggests that the steep mica fabric in central Mainland formed towards
479 the end of garnet growth, and that the Lu-Hf garnet age represents prograde growth, whereas
480 the Sm-Nd age represents cooling from this peak metamorphism due to differences in closure
481 temperatures of the two systems.

482 An amphibolite collected from the Valayre granitic orthogneiss on Lunna Ness in eastern
483 Mainland (AB08-18) yields a Lu-Hf age of 496.2 ± 5.4 Ma for the three garnets alone (MSWD =
484 0.07; N=3). No flux-fused WR is available for this sample, and individual two-point garnet-ttWR
485 ages for the three differently-coloured garnet fractions increase with increasing $^{176}\text{Lu}/^{177}\text{Hf}$ (0.34
486 to 0.69) from 438 Ma (pink) to 469.6 ± 2.5 Ma (orange fraction). The ttWR digestion has Hf content
487 of about 40% of the expected Hf content based on Zr/40, so it may be that it is a reasonable
488 estimate of the WR Lu-Hf isotope system. If so, the 469.6 Ma age is likely to be the most robust
489 for this sample. No Sm-Nd age was determined. Several samples from Lunna Ness were dated by

490 Cutts et al. (2011), using LA-ICPMS U-Pb monazite dating. They concluded that there were
491 multiple phases of metamorphism in this area, with monazite growth at c. 913 Ma, c. 470 Ma,
492 and c. 460 Ma. Cutts et al. (2011) also constrained the peak metamorphic conditions for the
493 Caledonian phase (as opposed to the Neoproterozoic) of monazite growth to 10 kbar, 775°C.

494

495 ***Ages from Yell***

496 AB08-6, a garnet-pyroxene-amphibolite from a Neoarchaean basement inlier, yields a $1051.2 \pm$
497 3.2 Ma Lu-Hf age from an extremely radiogenic garnet, and a Sm-Nd age of 863.1 ± 3.6 Ma. The
498 lower Sm-Nd age probably reflects a later metamorphic event as c. 920 Ma in situ monazite ages
499 are reported from the Valayre Gneiss at Lunna Ness (Cutts et al. 2011), and from the Westing
500 Group on Unst (Cutts et al. 2009).

501 Amphibolite AB08-08 intrudes the host Yell Sound Group pelitic gneisses in northeastern
502 Yell and yields an early Ordovician Sm-Nd isochron age using both garnet fractions of 478.1 ± 2.3
503 Ma (MSWD=0.42, N=3), with both being highly radiogenic. The garnets have lower Lu/Hf ratios
504 than the ttWR, but the purple garnet yields a Lu-Hf age of 453.6 ± 5.1 Ma (MSWD=0.16 with both
505 WR samples), and the orange garnet yields a 2-point age of 442 ± 6 Ma with the fused WR. This
506 is the third sample in this study in which Lu-Hf ages are younger than Sm-Nd ages. The low
507 $^{176}\text{Lu}/^{177}\text{Hf}$ of the garnets (0.15-0.17), together with the isochron age calculated with the
508 implausible ttWR, suggest that these Lu-Hf ages may not be meaningful. The large (≥ 6 mm)
509 garnets in AB08-08 have slightly curved inclusion trails, and are wrapped by the main fabric in
510 the rock which is dominated by amphibole.

511 On the north coast at the Sands of Breckon, a pelitic gneiss from within the Yell Sound
512 Group (AB08-04) yields a slightly younger middle Ordovician Sm-Nd age of 467.2 ± 1.4 Ma. No
513 Lu-Hf data are available from this sample. The dated garnets are wrapped by a steep D2 foliation
514 and rimmed by pressure shadows that are elongate parallel to a gently-plunging L2 mineral and
515 stretching lineation. A lower limit on the age of the D2 fabrics here is provided by an Rb-Sr white
516 mica age of 459.4 ± 1.4 Ma obtained from a folded syn-kinematic pegmatite at the same locality
517 (Walker et al. 2016). D2 deformation in NE Yell is thus constrained to have occurred between c.
518 468 Ma and c. 460 Ma.

519

520 ***Ages from Unst and Fetlar***

521 Two orange and two pink garnet fractions were analysed from AB08-14, a pelitic gneiss from the
522 Westing Group of Unst. A Lu-Hf errorchron of 837 ± 42 Ma (MSWD = 57) can be obtained from
523 the three most radiogenic garnets and the flux-fused WR, while the Sm-Nd data yield an
524 errorchron of 585 ± 17 Ma (MSWD = 24, N=5). Neither colour garnet yields an isochron for either
525 Lu-Hf or Sm-Nd, but pink garnet-WR two-point Lu-Hf ages are nearly within error at 837 and 846
526 Ma, while the orange garnets yield 759 and 815 Ma. $^{176}\text{Lu}/^{177}\text{Hf}$ ratios in the garnets are fairly
527 low (0.18-0.27), lower than the ttWR sample. The three most radiogenic garnets (two pink, one
528 orange) lie on a Lu-Hf isochron of age 907 ± 14 Ma, MSWD = 0.26. The garnets have moderate
529 $^{147}\text{Sm}/^{144}\text{Nd}$ ratios (0.39-0.63) and give fairly consistent two-point ages from 573 ± 4 to 589 ± 3
530 Ma. There is no indication of older Sm-Nd ages for the pink garnets. Three of the garnets (all
531 except the least radiogenic) yield a Sm-Nd isochron of 607 ± 6 Ma, MSWD = 0.02. The Lu-Hf data,
532 especially the 3-garnet age, are consistent with the c. 930 Ma Tonian metamorphic event
533 identified in the Westing Group by Cutts et al. (2009), while the lower Sm-Nd ages may reflect a
534 late Proterozoic event or partial Caledonian reworking.

535 The garnets of metabasite SW15-07 yield the oldest Caledonian age determined in this
536 study. The sample comes from the metamorphic sole of the upper thrust sheet of the Shetland
537 Ophiolite Complex on Fetlar. At outcrop, the lithology carries a strong, near horizontal
538 deformation fabric, parallel to the contact with the overlying metaharzburgite. The lithology
539 appears to have distinct relict garnet-clinopyroxene layers, which have a pronounced boundary,
540 defined by titanite, with a stable garnet-amphibole assemblage. Trace-element profiles across
541 garnets determined by LA-ICPMS show that concentrations of the HREE, including Lu, are slightly
542 higher at the centre of the garnet crystals compared to the rims, although the crystals do not
543 show a bell-shaped Lu profile which would be expected for a sample recording prograde growth.
544 This may indicate some degree of diffusion of the HREE due to high-temperature metamorphism,
545 or that the garnet analysed for trace-elements was not cut precisely down the centre of the
546 crystal. Garnet-clinopyroxene thermometry was undertaken on this lithology by Spray (1988),
547 which yielded temperatures of c. 750°C on the peak temperature assemblage. Garnets,

548 pyroxenes, and amphiboles were separated from the two assemblages, using a saw to separate
549 the two assemblages, to resolve any potential differences in the timing of formation of the
550 garnet-pyroxene and garnet-amphibole assemblages. A Lu-Hf isochron of 491.4 ± 5.5 Ma (N=4,
551 MSWD 4.1) is defined by both garnet fractions, the amphibole, and pyroxene. This indicates that
552 the prograde and retrograde assemblages formed within the uncertainty of the isochron.

553 The remaining analyses from Unst and Fetlar were all obtained from samples of the East
554 Mainland Succession. The pink garnet fraction of pelite AB08-15 from west Unst yields early
555 Ordovician Lu-Hf and Sm-Nd ages of 484.5 ± 1.5 Ma and 472.3 ± 4.8 Ma respectively, and we
556 interpret this age as an early garnet population, perhaps garnet cores, based on thin-section and
557 hand-specimen observations of garnet colouration. The presence of kyanite in the cores of these
558 garnets indicates that this age relates to an early phase of kyanite-grade metamorphism. The
559 sample was collected from the same lithology (although not the same outcrop) as sample KSH07-
560 12 from Cutts et al. (2011), who constrained the age and peak metamorphic conditions to 7.5
561 Kbar and 630°C at 462 ± 10 Ma. Their age was determined by LA-ICPMS U-Pb dating of monazite
562 inclusions within the rim of garnet. They did note that the garnets in this sample had distinct
563 cores and rims, with different peak assemblages, but could not date the cores due to a lack of
564 monazite inclusions. The orange garnet fraction of this pelite (AB08-15), which we interpret as
565 the garnet rims, yields middle to late Ordovician ages (Lu-Hf 462.9 ± 1.7 Ma, Sm-Nd 455.4 ± 3.5),
566 21 to 17 Ma younger than the (pink) garnet cores. The rim ages are within error of the 462 ± 10
567 Ma U-Pb monazite age determined by Cutts et al. (2011), which is consistent with their location
568 in the garnet rims.

569 A pelitic gneiss from west Fetlar (sample SW12-14) was collected from approximately the
570 same structural level as AB08-15 on Unst (Fig. 4), and yields an identical Lu-Hf isochron age of
571 484.5 ± 1.4 Ma (n=5; MSWD = 1.6), indicating that the timing of garnet growth in this unit was
572 synchronous with the equivalent unit in Unst. There appears to be no difference in the growth
573 times of the pink and orange garnet fractions, which were separated based on colour when
574 picking, given that they all fall on the same isochron with low MSWD. However, these garnets
575 yield younger Sm-Nd ages. The first pair analysed yielded a late Ordovician isochron age of 453.7
576 ± 3.8 (N=3, MSWD 0.64), within error of the rim Sm-Nd age of AB08-15. Orange and pink garnets

577 analysed in a second analytical batch give an older age of 472 ± 10 Ma, but these have lower
578 Sm/Nd and were not analysed at the same time as the WR, so it is hard to make accurate
579 corrections for instrumental drift. The mica fabrics wrapping the garnets in this sample were
580 dated using Rb-Sr on both white mica and biotite, yielding ages of 468.9 ± 1.4 Ma and 451.2 ± 1.4
581 Ma respectively (Walker et al. 2016).

582 Three garnet fractions and three separate fused WR samples from pelite SW12-16, from
583 northeast Unst, define a Lu-Hf isochron age of 470.0 ± 1.2 Ma ($n=4$; MSWD: 1.1). Peak pressure-
584 temperature constraints of 7.5 kbar, 550°C have been calculated on the same unit (Cutts et al.
585 2011). Given that the LA-ICPMS garnet traverse for this sample shows typical prograde Lu zoning
586 pattern of a bell-shaped central peak (Fig. 5C), and the relatively low temperature determined in
587 Cutts et al. (2011) it is very likely that these metamorphic conditions were reached at c. 470 Ma,
588 and that the age represents garnet growth.

589 A late Ordovician Lu-Hf garnet age was determined from SW12-15, a pelitic schist from
590 western Unst that yielded a Lu-Hf age of 452.0 ± 1.4 Ma and a Sm-Nd age of 454.3 ± 7.5 Ma.
591 Porphyroblasts of staurolite and chloritoid in this sample overprint the foliation that wraps the
592 garnets, indicating that post-deformational metamorphism reached at least (lower) amphibolite
593 facies after garnet growth at c. 452 Ma (Fig. 5D).

594 The Saxa Vord pelite SW12-16 in NE Unst gives a Sm-Nd isochron age of 430.4 ± 4.2 Ma
595 ($N=4$, MSWD=0.88), despite the same garnets giving a Lu-Hf isochron age of 470.0 ± 1.2 Ma. This
596 time gap suggests that a second Silurian metamorphic event re-equilibrated garnet Nd but not
597 Hf. The fact that 3 different garnet fractions lie on each isochron suggests that we are not
598 preferentially sampling Lu-rich cores to obtain the older age.

599

600 **Discussion and regional correlations**

601

602 ***Pre-Caledonian events in Shetland***

603 The Lu-Hf age of c. 1050 Ma obtained from reworked Neoproterozoic basement in NE Yell (sample
604 AB-08-06) predates deposition of the Yell Sound and Westing groups (Cutts et al. 2009; Jahn et
605 al 2017). It compares with Sm-Nd mineral isochron ages of c. 1082 Ma and c. 1010 Ma for eclogite

606 facies metamorphism of the Eastern Glenelg basement inlier in the Caledonides of NW Scotland,
607 which has been attributed to the Grenvillian orogeny (Sanders et al. 1984). It seems reasonable
608 to assign the new age from NE Yell to the same tectonic event which in Scotland likely resulted
609 from the collision of Baltica and Laurentia during the assembly of Rodinia (Li et al. 2008; Strachan
610 et al. 2020a). The 3-garnet isochron age of 907 ± 14 Ma obtained from the Westing Group (sample
611 AB-08-14) is consistent with the 938-925 Ma span of zircon and monazite ages reported by Cutts
612 et al. (2009) and attributed to the Renlandian event of Cawood et al. (2010).

613 The Lu-Hf ages of c. 622-606 Ma and the Sm-Nd age of 617 ± 9 Ma obtained from the
614 Walls Metamorphic Series (samples SW15-06 and 15-03) are more problematic as they suggest
615 that these rocks were undergoing high-grade metamorphism at the same time as the East
616 Mainland Succession was being deposited in an extensional basin immediately east of the Walls
617 Boundary Fault (Prave et al. 2009). The mismatch could be explained in one of two ways. Either
618 the Walls Metamorphic Series or the East Mainland Succession is grossly allochthonous and rests
619 on an as-yet-undetected major thrust, or alternatively there has been substantial displacement
620 along the Walls Boundary Fault. It is noteworthy that Slagstad et al. (2020) report a similar c. 623
621 Ma age for high-grade metamorphism within the Uppermost Allochthon in Norway which is
622 believed to have a Laurentian parentage. The eastern Laurentian margin is widely thought to
623 have been under extension during the Ediacaran breakup of Pannotia, so the tectonic significance
624 of c. 620 Ma metamorphic events represents an unresolved problem.

625 The c. 510 Ma Lu-Hf age obtained from the Walls Metamorphic Series (sample SW-15-01)
626 is easier to explain as there is no reason to suppose that it overlaps with the depositional history
627 of the East Mainland Succession. Furthermore, it is only 20 Ma older than the onset of ophiolite
628 obduction (see below) and could conceivably simply indicate that the Grampian I event was more
629 complex and protracted than envisaged in current tectonic models. This solution is supported by
630 the recognition of an early phase of thrusting at c. 515 Ma in the Uppermost Allochthon of
631 Scandinavia (Slagstad et al. 2020).

632

633 ***Onset and duration of Grampian I metamorphism in Shetland***

634 The garnet ages determined in this study show that the dominant period of garnet growth in
635 Shetland related to Grampian (Ordovician) accretionary events. The new data are consistent with
636 the ages obtained in Shetland in recent geochronological studies using U-Pb and Rb-Sr isotopic
637 systems (Cutts et al. 2011; Crowley & Strachan 2015; Walker et al. 2016; Jahn et al. 2017). The
638 Lu-Hf isochron age of 491.4 ± 5.5 Ma obtained from the metamorphic sole of the ophiolite on
639 Fetlar consists of minerals that are not in metamorphic equilibrium. This suggests that the change
640 from upper to middle amphibolite grade happened within the age uncertainty of 5.5 Ma. Titanite
641 porphyroblasts along the boundaries of the regions that have preserved higher temperature
642 pyroxene-bearing assemblages and those that have been completely recrystallized to amphibole
643 (Fig. 5) suggest that a calcic fluid was interacting with the rock at this time, and contributed to
644 the mineralogical changes (Spray 1988). The age most likely relates to high temperature
645 metamorphism of the subducting oceanic slab that formed the protolith of the metamorphic sole
646 (Spray 1988). It is within analytical uncertainty of the 484 ± 4 Ma U-Pb zircon age obtained by
647 Crowley & Strachan (2015) from the same unit on Unst, which we suggest probably relates to
648 subsequent decompression melting during exhumation and obduction. Similar ages are found
649 within the Highland Border Ophiolite in SW Mainland Scotland, where U-Pb zircon ages of $499 \pm$
650 8 Ma have been interpreted as dating magmatism, and $^{40}\text{Ar}/^{39}\text{Ar}$ dating of hornblende and
651 muscovite yield 490 ± 4 Ma and 488 ± 1 Ma ages respectively, and relate to the timing of
652 obduction (Chew et al. 2010).

653 The age of (pink) garnet cores from western Unst pelite, AB08-15, and the metamorphic
654 conditions calculated on the same unit by Cutts et al. (2011), indicate that prograde Barrovian
655 metamorphism of 7 kbar and 630°C was underway in this part of Shetland as early as 484.5 ± 1.5
656 Ma. This suggests that growth of a significant orogenic wedge took place within ~ 6 Ma of the
657 formation of the metamorphic sole of the ophiolite. Near identical garnet ages are also recorded
658 from the same structural level on Fetlar, and in rims of late Proterozoic garnets, and by Sm-Nd,
659 in the Walls Metamorphic Series. Slightly younger ages of 478-480 Ma in Yell, east Mainland and
660 in the Eastern gneisses of North Roe indicate that this metamorphic event was widespread
661 through Shetland. This suggests that the onset of peak Grampian metamorphism occurred
662 slightly earlier than in the Dalradian Supergroup in mainland Scotland, where peak

663 metamorphism occurred between 473 ± 3 Ma and 465 ± 3 Ma, giving a maximum possible
664 duration of 14 Ma (Oliver et al. 2000; Baxter et al. 2002; Viete et al. 2013).

665 Peak Grampian I metamorphism in Shetland occurred over a duration of 33 Ma based on
666 garnet core ages that span 491.4 ± 5.5 Ma to 466.3 ± 2.2 Ma, significantly longer than in mainland
667 Scotland. Both age constraints are Lu-Hf garnet ages, and are therefore directly comparable,
668 bypassing any potential differences between the Lu-Hf and Sm-Nd garnet systems (e.g. Bloch et
669 al. 2015). Many of the samples that record Grampian ages exhibit prograde zoning in trace-
670 element (HREE) LA-ICPMS traverses, which suggests that these Lu-Hf ages relate to the prograde
671 growth of garnet. The difference in the timing of Grampian peak metamorphism between
672 Shetland and the Grampian Highlands shows that, in Shetland, this event is longer in duration
673 and not just earlier than in mainland Scotland.

674 There are strong similarities between the Grampian I event in Shetland and coeval events
675 preserved along strike in Scandinavia (Fig. 1A). It has long been recognised that the highest
676 structural units in central Norway, grouped as the 'Uppermost Allochthon' (Fig. 1A; Roberts &
677 Gee 1985), represent a fragment of Laurentia that was emplaced as a composite terrane onto
678 the down-going Baltican plate during Scandian continental collision (Roberts 2003; Roberts et al.
679 2007; Corfu 2014 and references therein). The 'Uppermost Allochthon' contains various
680 metasedimentary units that have been deduced to have a Laurentian parentage, partly on
681 palaeontological grounds (e.g. Bruton & Brockelie 1980), and record deformation and
682 metamorphism during the Lower Ordovician (480-475 Ma) prior to emplacement of arc-related
683 plutons (470-455 Ma) (e.g. Nordgulen et al. 1993; Yoshinobu et al. 2002; Barnes et al. 2007). In
684 SW Norway, the Karmøy-Bergen ophiolites (Fig 1A) and associated island arc sequences are also
685 thought to have originated in a peri-Laurentian setting (Pedersen & Hertogen 1990; Pedersen &
686 Dunning 1997). The metasedimentary rocks of the Jæren nappe (Fig 1A) have Laurentian affinities
687 and were affected by eclogite facies metamorphism at c. 470 Ma (Smit et al. 2010). The Lower
688 Ordovician tectonothermal events recorded within these structurally highest nappes have been
689 correlated directly with the Grampian orogeny of Scotland (Roberts 2003; Roberts et al. 2007)
690 and clearly correspond closely in timing to the 'Grampian I' event in Shetland.

691

692 ***Evidence for the Grampian II event in Shetland***

693 The late Ordovician ages reported here significantly widen the geographical extent of the
694 Grampian II event within the Scottish Caledonides. However, the differentiation between
695 Grampian I and II events is less clear than in mainland Scotland. In Shetland, Lu-Hf data do not
696 show any age gaps greater than 4 Ma between 453 and 484 Ma. However, there is a gap from
697 466.3 to 458.8 Ma if only core ages are considered, which may reflect the gap between Grampian
698 I and II. Within this gap there are only two Lu-Hf rim ages, and one Sm-Nd rim age. In Shetland,
699 evidence of garnet growth during the late Ordovician is found on both sides of the Walls
700 Boundary Fault. In North Roe, garnets of this age are found in two samples (AB08-11 and AB08-
701 13; 446.5 and 456.7 Ma), east of and structurally above the Wester Keolka Shear Zone. In
702 contrast, samples (AB08-12 and SW13-08) collected 250m and 130m southeast from the previous
703 samples, and also from the Eastern Gneisses, but from amphibolites rather than pelites, yield
704 Grampian I ages (479.6 and 466.3 Ma respectively). The difference in ages may indicate that the
705 two samples are separated by a cryptic tectonic break. The Hillswick pelite, SW13-27, also yields
706 a core age (458.8 Ma) on the boundary between late and middle Ordovician, and a clearly late
707 Ordovician rim age (453.0 Ma). A Late Ordovician age of 452.0 ± 1.4 Ma is also recorded in western
708 Unst, and can be attributed to the Grampian II event. Pressure-temperature estimates for
709 western Unst range between 7.5 – 8.5 kbar, and 630 – 650°C (Cutts et al. 2011). This suggests
710 that regional metamorphism in Unst occurred at both *c.* 450 Ma and *c.* 470 Ma. There is also
711 some evidence for late Ordovician garnet growth on Yell (sample AB08-8), although the garnets
712 from this sample are relatively unradiogenic.

713 There is evidence of a possible structural control on the locations of Grampian II garnet
714 growth. Post-Grampian I metamorphism only occurs where the dominant tectonic fabrics are
715 shallowly dipping (i.e. not in the Central Steep Zone in Central Shetland and Yell, Fig. 2), which
716 may reflect that these were easier to reactivate during subsequent tectonic events. Set against
717 this, sample AB08-18 was obtained from an area of steeply-dipping fabrics in the Lunna Ness
718 peninsula (Fig. 4) and yielded a Lu-Hf age of *c.* 449 Ma. However, this anomaly might indicate that
719 some fabric steepening occurred *after c.* 450-445 Ma. Areas with shallowly-dipping fabrics do not
720 exclusively record later Caledonian events as there are several examples of these west of the

721 Walls Boundary Fault and in the footwall of the Shetland Ophiolite Complex in both Unst and
722 Fetlar where only c. 480-470 Ma garnet ages have been recorded.

723 Metamorphic events of broadly the same age have been recorded along strike of Shetland
724 in the Uppermost Allochthon of Scandinavia, for example the c. 450 Ma eclogite facies event of
725 Corfu et al. (2003). One possibility is that here the Late Ordovician event(s) resulted from the
726 accretion to Laurentia of the outermost segments of a hyper-extended Baltican continental
727 margin (Jakob et al. 2019).

728

729 ***Scandian garnet growth in Shetland***

730 Our data provides evidence of Silurian metamorphism on both sides of the Walls Boundary Fault.
731 The 427 Ma Lu-Hf age obtained from reworked Archaean basement between the Uyea and
732 Wester Keolka shear zones is only slightly older than the Rb-Sr muscovite ages of c. 416 Ma and
733 c. 410 Ma yielded by the same orthogneisses c. 2 km farther west (Walker et al. 2016). The
734 consistency of the two data sets provides an additional indication that the widespread reworking
735 of basement here occurred at least in part during the Scandian orogenic event. However, if garnet
736 grade metamorphic conditions prevailed during the Silurian, it is difficult to understand why c.
737 720-700 Ma Rb-Sr muscovite ages recorded from the vicinity of the Wester Keolka Shear Zone
738 (Walker et al. 2016) only 300 m structurally higher were not reset. Further isotopic investigations
739 are needed to resolve this issue. The Sm-Nd age of 430 Ma recorded in NE Unst is also consistent
740 with Scandian metamorphism, and published Rb-Sr mica ages of 440-430 Ma from Unst (Walker
741 et al. 2016).

742 The Silurian to Lower Devonian age indicated for Scandian deformation and
743 metamorphism in Shetland overlaps with that established along strike in both the Northern
744 Highland Terrane of mainland Scotland (Dallmeyer et al. 2001; Kinny et al. 2003; Goodenough et
745 al. 2011; Mako et al. 2019; Strachan et al. 2020b) and the thrust allochthons of Scandinavia (Corfu
746 2014).

747

748 ***Significance of the Walls Boundary Fault***

749 Substantial displacements have been proposed for the Great Glen Fault in mainland Scotland,
750 which has been correlated with the Walls Boundary Fault (Flinn 1961, 1977, 1992; Watts et al.
751 2007). Both terranes either side of the Great Glen Fault were affected by Grampian I deformation
752 and metamorphism (Kinny et al. 1999; Cutts et al. 2010; Bird et al. 2013), but evidence for the
753 Scandian orogenic event and Grampian II episode are restricted to the Northern Highland Terrane
754 (Kinny et al. 2003). Because the Scandian orogeny is attributed to the collision of Laurentia and
755 Baltica, it is thought that the Northern Highland Terrane must have been located opposite
756 southern Norway during plate collision, and was then displaced sinistrally along the Great Glen
757 Fault by c.700-500 km to juxtapose it against the Grampian Terrane (Coward 1990; Dallmeyer et
758 al. 2001; Dewey & Strachan 2003; Strachan et al. 2020b). By contrast, there does not appear to
759 be any significant difference in the timing of Caledonian metamorphic events either side of the
760 Walls Boundary Fault (Fig. 6), although this is not unexpected given that any northern extension
761 of the Great Glen Fault would at some point be separating crustal blocks that were both affected
762 by the Scandian orogeny. However, the potential incompatibility of Ediacaran events either side
763 of the Walls Boundary Fault alluded to above may be indicative of significant lateral displacement
764 and requires further investigation.

765

766 **Conclusions**

767 1. The Lu-Hf and Sm-Nd garnet ages presented here indicate a complex Neoproterozoic
768 and Lower Palaeozoic orogenic history for the Laurentian Caledonides of Shetland.

769 2. A Lu-Hf age of c. 1050 Ma obtained from Neoproterozoic basement in NE Yell compares
770 with the timing of eclogite facies metamorphism of basement in the Caledonides of NW Scotland
771 during the Grenvillian orogeny. We assign the new age from NE Yell to the same tectonic event
772 which in Scotland probably resulted from the collision of Baltica and Laurentia during the
773 assembly of Rodinia (Li et al. 2008; Strachan et al. 2020a).

774 3. A 3-garnet Lu-Hf isochron age of 907 ± 14 Ma obtained from the Westing Group is
775 consistent with the 938-925 Ma span of published zircon and monazite ages and attributed to
776 the Renlandian accretionary orogenic event of Cawood et al. (2010).

777 4. Ediacaran garnet ages of c. 622-606 Ma obtained from the Walls Metamorphic Series
778 are more difficult to explain because the eastern margin of Laurentia is thought to have been in
779 extension at that time during the break-up of Pannotia. However, similar metamorphic ages have
780 been recorded from Laurentian-derived allochthons in Scandinavia, suggesting a more
781 widespread event that is not yet understood fully.

782 5. Lu-Hf garnet ages of c. 510 Ma obtained from the Walls Metamorphic Series and c. 491
783 from metamorphic sole of the Shetland ophiolite are interpreted as corresponding to the onset
784 of Grampian I orogenic activity which has been widely documented in mainland Scotland, Ireland
785 and in the Laurentian-derived allochthons of Scandinavia. Peak metamorphism was reached by
786 c. 485 Ma, which is c. 10 Ma earlier than in mainland Scotland. There is widespread evidence of
787 garnet growth on both sides of the Walls Boundary Fault until c. 466 Ma which also indicates a
788 more protracted Grampian event in Shetland.

789 6. Lu-Hf and Sm-Nd ages ranging between c. 459 and c. 442 Ma are attributed to the Late
790 Ordovician Grampian II event, significantly widening its geographical extent from mainland
791 Scotland and providing linkage with similar-age events in the Laurentian-derived allochthons of
792 Scandinavia. Garnet growth of this age is recorded on both sides of the Walls Boundary Fault and
793 appears to have been focused in areas where pre-existing foliations were gently-inclined and
794 thus may have been relatively easily reworked.

795 7. Lu-Hf and Sm-Nd ages of c. 430 Ma obtained from two samples in Shetland are
796 interpreted to correspond to the Scandian orogeny. The relative paucity of Silurian ages suggests
797 that the Scandian orogenic event here was not characterized by sufficiently high temperatures
798 and pressures to result in widespread garnet growth.

799 8. There is no significant difference in the timing of Caledonian orogenic events either
800 side of the Walls Boundary Fault, although this need not preclude linkage with the Great Glen
801 Fault. However, the incompatibility of Ediacaran events either side of the Walls Boundary Fault
802 may indicate significant lateral displacement and requires further investigation.

803

804 **Acknowledgements**

805 SW acknowledges receipt of a NERC PhD fellowship. The participants of the 2015 MSG field
806 workshop are thanked for discussion in the field. Thanks are also due to Robert Anczkiewicz for
807 provision of laboratory facilities in Kraków, and to Wolfgang Müller for help with the RHUL laser
808 ablation facility. Stephen Daly and Andrew Carter are thanked for discussion and comments that
809 improved an early draft of this manuscript. Thanks also to Graham Leslie and an anonymous
810 reviewer for their helpful and constructive reviews, and to Brendan Murphy for his editorial
811 comments.

812

813 **References**

814 Anczkiewicz, R., & Thirlwall, M. F. (2003). Improving precision of Sm-Nd garnet dating by H₂SO₄ leaching: a simple
815 solution to the phosphate inclusion problem. *Journal of the Geological Society, London*, *220*, 83–91.

816 Anczkiewicz, R., Platt, J. P., Thirlwall, M. F., & Wakabayashi, J. (2004). Franciscan subduction off to a slow start:
817 evidence from high-precision Lu–Hf garnet ages on high grade-blocks. *Earth and Planetary Science Letters*,
818 *225*(1–2), 147–161. <https://doi.org/10.1016/j.epsl.2004.06.003>

819 Andrews, I. J. (1985). The deep structure of the Moine Thrust, southwest of Shetland. *Scottish Journal of Geology*,
820 *21*(2), 213–217. <https://doi.org/10.1144/sjg21020213>

821 Barnes, C. G., Frost, C. D., Yoshinobu, A. S., McArthur, K., Barnes, M. A., Allen, C. M., Prestvik, T. (2007). Timing of
822 sedimentation, metamorphism, and plutonism in: The Helgeland Nappe Complex, north-central Norwegian
823 Caledonides. *Geosphere*, *3*(6), 683–703. <https://doi.org/10.1130/GES00138.1>

824 Baxter, E. F., Ague, J. J., & Depaolo, D. J. (2002). Prograde temperature – time evolution in the Barrovian type –
825 locality constrained by Sm / Nd garnet ages from Glen Clova, Scotland. *Journal of the Geological Society*,
826 *London*, *159*(1985), 71–82.

827 Baxter, E. F., & Scherer, E. E. (2013). Garnet Geochronology: Timekeeper of Tectonometamorphic Processes.
828 *Elements*, *9*(6), 433–438. <https://doi.org/10.2113/gselements.9.6.433>

829

830 Baxter, E. F., Caddick, M. J., & Dragovic, B. (2017). Garnet: A Rock-Forming Mineral Petrochronometer. *Reviews in*
831 *Mineralogy and Geochemistry*, *83*(1), 469–533. <https://doi.org/10.2138/rmg.2017.83.15>

832 Biejat, S., Strachan, R. A., Storey, C. D., & Lancaster, P. J. (2018). Evidence for an Early Silurian Synorogenic Basin
833 Within the Metamorphic Hinterland of the North Atlantic Caledonides: Insights From the U-Pb Zircon
834 Geochronology of the Funzie Conglomerate, Shetland, Scotland. *Tectonics*, 1–20.
835 <https://doi.org/10.1029/2018TC005050>

836 Bird, A. F., Thirlwall, M. F., Strachan, R. A., Manning, C. J., (2013). Lu – Hf and Sm – Nd dating of metamorphic garnet:
837 evidence for multiple accretion events during the Caledonian orogeny in Scotland. *Journal of the Geological*
838 *Society, London*, 170, 301–317. <https://doi.org/10.1144/jgs2012-083.Lu>

839 Bird, A.F., Cutts, K.A., Strachan, R.A., Thirlwall, M. & Hand, M. 2018. First evidence of Renlandian (c. 950 Ma) orogeny
840 in Mainland Scotland: implications for circum-North Atlantic correlations and the status of the Moine
841 Supergroup. *Precambrian Research*, 350, 283-294, doi: 10.1016/j.precamres.2017.12.019.

842 Bloch, E., & Ganguly, J. (2015). 176Lu–176Hf geochronology of garnet II: numerical simulations of the development
843 of garnet–whole-rock 176Lu–176Hf isochrons and a new method for constraining the thermal history of
844 metamorphic rocks. *Contributions to Mineralogy and Petrology*, 169. [https://doi.org/10.1007/s00410-015-](https://doi.org/10.1007/s00410-015-1115-x)
845 1115-x

846 Bloch, E., Ganguly, J., Hervig, R., & Cheng, W. (2015). 176Lu–176Hf geochronology of garnet I: experimental
847 determination of the diffusion kinetics of Lu³⁺ and Hf⁴⁺ in garnet, closure temperatures and geochronological
848 implications. *Contributions to Mineralogy and Petrology*, 169. <https://doi.org/10.1007/s00410-015-1109-8>

849 Bruton, D. L., & Bockelie, J. F. (1980). Geology and Paleontology of the Høllonda area, western Norway, a fragment
850 of North America? *Virginia Polytechnic Institute State University Department of Science Memo*, 2, 41-55.

851 Cannat, M. (1989). thrusting Late Caledonian northeastward Islands , U.K . -Reply ophiolite thrusting in the Shetland,
852 396–397.

853 Cawood, P.A., Strachan, R.A., Cutts, K.A., Kinny, P.D., Hand, M. & Pisarevsky, S. 2010. Neoproterozoic orogeny along
854 the margin of Rodinia: Valhalla orogen, North Atlantic. *Geology*, 38, 99-102, doi: 10.1130/G30450.1.

855 Cawood, P.A., Strachan, R.A., Merle, R.E., Millar, I.L., Loewy, S.L., Dalziel, I.W., Kinny, P.D., Jourdan, F., Memchin, A.A.
856 & Connelly, J.N. 2015. Neoproterozoic to early Palaeozoic extensional and contractional history of East
857 Laurentian margin sequences. the Moine Supergroup, Scottish Caledonides. *Geological Society of America*
858 *Bulletin*, 127, 349-371, doi: 10.1130/B31068.1.

- 859 Chew, D. M., Daly, J. S., Magna, T., Page, L. M., Kirkland, C. L., Whitehouse, M. J., & Lam, R. (2010). Timing of ophiolite
860 obduction in the Grampian orogen. *Bulletin of the Geological Society of America*, 122(11), 1787–1799.
861 <https://doi.org/10.1130/B30139.1>
- 862 Corfu, F., Ravna, E. J. K., & Kullerud, K. (2003). A Late Ordovician U-Pb age for the Tromsø Nappe eclogites Uppermost
863 Allochthon of the Scandinavian Caledonides. *Contributions to Mineralogy and Petrology*, 145(4), 502–513.
864 <https://doi.org/10.1007/s00410-003-0466-x>
- 865 Corfu, F., Andersen, T. B., & Gasser, D. (2014). The Scandinavian Caledonides: main features, conceptual advances
866 and critical questions. *Geological Society, London, Special Publications*, 390(1), 9–43.
867 <https://doi.org/10.1144/SP390.25>
- 868 Coward, M. P. (1990). The Precambrian, Caledonian and Variscan framework to NW Europe. *Geological Society,*
869 *London, Special Publications*, 55(1), 1–34. <https://doi.org/10.1144/GSL.SP.1990.055.01.01>
- 870 Crowley, Q. G., & Strachan, R. A. (2015). U-Pb zircon constraints on obduction initiation of the Unst Ophiolite: an
871 oceanic core complex in the Scottish Caledonides? *Journal of the Geological Society, London*, 172(3), 279–282.
872 <https://doi.org/10.1144/jgs2014-125>
- 873 Cutts, K. A., Hand, M., Kelsey, D. E., Wade, B., Strachan, R. a., Clark, C., & Netting, a. (2009). Evidence for 930 Ma
874 metamorphism in the Shetland Islands, Scottish Caledonides: implications for Neoproterozoic tectonics in the
875 Laurentia-Baltica sector of Rodinia. *Journal of the Geological Society, London*, 166(6), 1033–1047.
876 <https://doi.org/10.1144/0016-76492009-006>
- 877 Cutts, K. A., Kinny, P. D., Strachan, R. A., Hand, M., Kelsey, D. E., Emery, M., Leslie, A. G. (2010). Three metamorphic
878 events recorded in a single garnet: Integrated phase modelling, in situ LA-ICPMS and SIMS geochronology from
879 the Moine Supergroup, NW Scotland. *Journal of Metamorphic Geology*, 28(3), 249–267.
880 <https://doi.org/10.1111/j.1525-1314.2009.00863.x>
- 881 Cutts, K. A., Hand, M., Kelsey, D. E., & Strachan, R. A. (2011). P-T constraints and timing of Barrovian metamorphism
882 in the Shetland Islands, Scottish Caledonides: implications for the structural setting of the Unst ophiolite.
883 *Journal of the Geological Society, London*, 168(6), 1265–1284. <https://doi.org/10.1144/0016-76492010-165>
- 884 Dallmeyer, R. D., Strachan, R. A., Rogers, G., Watt, G. R., & Friend, C. R. L. (2001). Dating deformation and cooling in
885 the Caledonian thrust nappes of north Sutherland, Scotland: insights from $^{40}\text{Ar} / ^{39}\text{Ar}$ and Rb – Sr chronology.
886 *Journal of the Geological Society, London*, 158, 501–512.

- 887 Dempster, T. J., Hay, D. C., & Bluck, B. J. (2004). Zircon growth in slate. *Geology*, 32(3), 221-224
- 888 Dewey, J. F., & Shackleton, R. M. (1984). A model for the evolution of the Grampian tract of the early Caledonides
889 and Appalachians. *Nature*, 312, 115–121.
- 890 Dewey, J. F., & Ryan, P. D. (1990). The Ordovician evolution of the South Mayo trough, western
891 Ireland. *Tectonics*, 9(4), 887-901
- 892 Dewey, J. F., & Strachan, R. A. (2003). Changing Silurian–Devonian relative plate motion in the Caledonides: sinistral
893 transpression to sinistral transtension. *Journal of the Geological Society, London*, 160, 219–229. Retrieved from
894 <http://jgs.lyellcollection.org/content/160/2/219.short>
- 895 Dewey, J. F., Dalziel, I. W. D., Reavy, R. J., & Strachan, R. A. (2015). The Neoproterozoic to Mid-Devonian evolution
896 of Scotland: a review and unresolved issues. *Scottish Journal of Geology*, 51(1), 5–30.
897 <https://doi.org/10.1144/sjg2014-007>
- 898 Dichiarante, A.M., Holdsworth, R.E., Dempsey, E.D., Selby, D., McCaffrey, K.J.W., Michie, U.M., Morgan, G. and
899 Bonniface, J., 2016. New structural and Re–Os geochronological evidence constraining the age of faulting
900 and associated mineralization in the Devonian Orcadian Basin, Scotland. *Journal of the Geological*
901 *Society*, 173(3), pp.457-473.
- 902 Flinn, D. (1958). on the Nappe Structure of North-East Shetland. *Quarterly Journal of the Geological Society, London*,
903 114(1–4), 107–136. <https://doi.org/10.1144/gsjgs.114.1.0107>
- 904 Flinn, D. (1961). Continuation of the Great Glen Fault beyond the Moray Firth. *Nature*, 191, 589–591.
- 905 Flinn, D., May, F., Roberts, J.L. & Treagus, J.E. (1972). A revision of the stratigraphic succession of the East Mainland
906 in Shetland. *Scottish Journal of Geology*, 8, 335-343.
- 907 Flinn, D. (1977). Transcurrent faults and associated cataclasis in Shetland. *Journal of the Geological Society, London*,
908 133(3), 231–247. <https://doi.org/10.1144/gsjgs.133.3.0231>
- 909 Flinn, D., Frank, P. L., Brook, M., & Pringle, I. R. (1979). Basement-cover relations in Shetland. *Geological Society*,
910 *London, Special Publications*, 8(1), 109–115. <https://doi.org/10.1144/GSL.SP.1979.008.01.09>
- 911 Flinn, D. (1985). The Caledonides of Shetland. In: Gee, D.G. & Sturt, B.A. (eds) *The Caledonide Orogen - Scandinavia*
912 *and Related Areas*. Wiley & Sons, New York, 1159-1172.

- 913 Flinn, D. (1988). The Moine rocks of Shetland. In: Winchester, J.A. (ed.) *Later Proterozoic Stratigraphy of the Northern*
914 *Atlantic Regions*. Blackie, Glasgow, 74-85.
- 915 Flinn, D. (1992). Late Caledonian northeastward ophiolite thrusting in the Shetland Islands, U.K. - Refutation, *216*,
916 387–389.
- 917 Flinn, D. (1993). Discussion on the location and history of the Walls Boundary fault and Moine thrust north and south
918 of Shetland. *Journal of the Geological Society, London*, **150**, 1003-1008.
- 919 Flinn, D. (1994). Geology of Yell and some neighbouring islands in Shetland. *Memoir of the British Geological Survey*,
920 Sheet 130 (Shetland). London, HMSO.
- 921 Flinn, D. (2001). The basic rocks of the Shetland Ophiolite Complex and their bearing on its genesis. *Scottish Journal*
922 *of Geology*, *37*(2), 79–96. <https://doi.org/10.1144/sjg37020079>
- 923 Flinn, D. (2007). The Dalradian rocks of Shetland and their implications for the plate tectonics of the northern Iapetus.
924 *Scottish Journal of Geology*, *43*(2), 125–142.
- 925 Flinn, D., Stone, P., & Stephenson, D. (2013). The Dalradian rocks of the Shetland Islands, Scotland. *Proceedings of*
926 *the Geologists' Association*, *124*(1–2), 393–409. <https://doi.org/10.1016/j.pgeola.2012.07.007>
- 927 Flinn, D. (2014). *Geology of Unst and Fetlar in Shetland: memoir for 1: 50 000 geological sheet 131 (Scotland) Unst*
928 *and Fetlar* (Vol. 131). British Geological Survey
- 929 Flinn, D., & Oglethorpe, R. J. D. (2005). A history of the Shetland Ophiolite Complex. *Scottish Journal of Geology*,
930 *41*(2), 141–148.
- 931 Ganguly, J., & Tirone, M. (1999). Diffusion closure temperature and age of a mineral with arbitrary extent of diffusion:
932 Theoretical formulation and applications. *Earth and Planetary Science Letters*, *170*(1–2), 131–140.
933 [https://doi.org/10.1016/S0012-821X\(99\)00089-8](https://doi.org/10.1016/S0012-821X(99)00089-8)
- 934 Garson, M. S., & Plant, J. (1973). Alpine Type Ultramafic rocks and episodic mountain building in the Scottish
935 Highlands. *Nature Physical Science*, *242*, 34–38.
- 936 Gee, D. G. (1975). A tectonic model for the central part of the Scandinavian Caledonides. *American Journal of Science*,
937 *275-A*, 468–515.

- 938 Goodenough, K. M., Millar, I., Strachan, R. A., Krabbendam, M., & Evans, J. A. (2011). Timing of regional deformation
939 and development of the Moine Thrust Zone in the Scottish Caledonides: constraints from the U-Pb
940 geochronology of alkaline intrusions. *Journal of the Geological Society, London*, 168(1), 99–114.
941 <https://doi.org/10.1144/0016-76492010-020>
- 942 Highton, A.J., Hyslop, E.K. & Noble, S.R. 1999. U—Pb zircon geochronology of migmatization in the northern Central
943 Highlands: evidence for pre-Caledonian (Neoproterozoic) tectonometamorphism in the Grampian Block,
944 Scotland. *Journal of the Geological Society, London*, 156, 1195-1204.
- 945 Jahn, I., Strachan, R. A., Fowler, M., Bruand, E., Kinny, P. D., Clark, C., & Taylor, R. J. M. (2017). Evidence from U – Pb
946 zircon geochronology for early Neoproterozoic (Tonian) reworking of an Archaean inlier in northeastern
947 Shetland, Scottish Caledonides. *Journal of the Geological Society, London*, 174, 217–232.
- 948 Jakob, J., Andersen, T.B. & Kjøl, H.J. 2019. A review and reinterpretation of the architecture of the South and South-
949 Central Scandinavian Caledonides – A magma-poor to magma-rich transition and the significance of the
950 reactivation of rift inherited structures. *Earth Science Reviews*, 192, 513-528.
- 951 Kinny, P. D., Friend, C. R. L., Strachan, R. A., Watt, G. R., & Burns, I. M. (1999). U–Pb geochronology of regional
952 migmatites in East Sutherland, Scotland: evidence for crustal melting during the Caledonian orogeny. *Journal*
953 *of the Geological Society*, 156(6), 1143-1152
- 954 Kinny, P. D., Strachan, R. A., Friend, C. R. L., Kocks, H., Rogers, G., & Patterson, B. (2003). U – Pb geochronology of
955 deformed metagranites in central Sutherland, Scotland: evidence for widespread late Silurian metamorphism
956 and ductile deformation of the Moine Supergroup during the Caledonian orogeny. *Journal of the Geological*
957 *Society, London*, 160, 259–269.
- 958 Kinny, P. D., Strachan, R. A., Fowler, M., Clark, C., Davis, S., Jahn, I., Taylor, R. J. M., Holdsworth, R. E., & Dempsey, E.
959 (2019). The Neoproterozoic Uyea Gneiss Complex, Shetland: an onshore fragment of the Rae Craton on the
960 European Plate. *Journal of the Geological Society, London*, 176(5), 847–862. [https://doi.org/10.1144/jgs2019-](https://doi.org/10.1144/jgs2019-017)
961 017
- 962 Kretz, R. 1983. Symbols for rock-forming minerals. *American Mineralogist*, 68, 277–279.
- 963 Lambert, R. S. J., & McKerrow, W. S. (1976). The Grampian Orogeny. *Scottish Journal of Geology*, 12(4), 271–292.
964 <https://doi.org/10.1144/sjg12040271>

- 965 Lapen, T. J., Johnson, C. M., Baumgartner, L. P., Mahlen, N. J., Beard, B. L., & Amato, J. M. (2003). Burial rates during
966 prograde metamorphism of an ultra-high-pressure terrane: An example from Lago di Cignana, western Alps,
967 Italy. *Earth and Planetary Science Letters*, 215(1–2), 57–72. [https://doi.org/10.1016/S0012-821X\(03\)00455-2](https://doi.org/10.1016/S0012-821X(03)00455-2)
- 968 Lancaster, P. J., Strachan, R. A., Bullen, D., Fowler, M., Jaramillo, M., & Saldarriaga, A. M. (2017). U – Pb zircon
969 geochronology and geodynamic significance of ‘Newer Granite ’ plutons in Shetland , northernmost Scottish
970 Caledonides. *Journal of the Geological Society, London*; 174 (3), 486-497
- 971 Leggett, J. K., McKerrow, W. S., & Eales, M. H. (1979). The Southern Uplands of Scotland: A Lower Palaeozoic
972 accretionary prism. *Journal of the Geological Society*, 136, 755–770. <https://doi.org/10.1144/gsjgs.136.6.0755>
- 973 Li, Z.-X., Bogdanova, S.V., Collins, A.S., Davidson, A., De Waele, B., Ernst, R.E., Fitzsimons, I.C.W., Fuck, R.A.,
974 Gladkochub, D.P., Jacobs, J., Karlstrom, K.E., Lu, S., Natapov, L.M., Pease, V., Pisarevsky, S.A., Thrane, K.,
975 Vernikovskiy, V., 2008. Assembly, configuration, and break-up history of Rodinia: A synthesis. *Precambrian*
976 *Research* 160, 179-210.
- 977 Lugmair, G. & Marti, K. (1978). Lunar initial $^{143}\text{Nd}/^{144}\text{Nd}$: Differential evolution of the lunar crust and mantle. *Earth*
978 *and Planetary Science Letters* 39(3), 349 – 357
- 979 Mako, C. A., Law, R. D., Caddick, M. J., Thigpen, J. R., Ashley, K. T., Cottle, J., & Kylander-Clark, A. (2019). Thermal
980 evolution of the Scandian Hinterland, Naver Nappe, Northern Scotland. *Journal of the Geological Society,*
981 *London*, 176(4), 669–688. <https://doi.org/10.1144/jgs2018-224>
- 982 Malone, S.J., McClelland, W.C., von Gosen, W., Piepjohn, K., 2017. The earliest Neoproterozoic magmatic record of
983 the Pearya terrane, Canadian high Arctic: Implications for Caledonian terrane reconstructions. *Precambrian*
984 *Research* 292, 323-349
- 985 McBride, J. H., & England, R. W. (1994). Deep seismic reflection structure of the Caledonian orogenic front west of
986 Shetland. *Journal of the Geological Society, London*, 151(1), 9–16. <https://doi.org/10.1144/gsjgs.151.1.0009>
- 987 Müller, W., Shelley, M., Miller, P., & Broude, S. (2009). Initial performance metrics of a new custom-designed ArF
988 excimer LA-ICPMS system coupled to a two-volume laser-ablation cell. *Journal of Analytical Atomic*
989 *Spectrometry*, 24(2), 209. <https://doi.org/10.1039/b805995k>
- 990 Mykura, W. 1976. Orkney and Shetland. *Institute of Geological Sciences Memoir*, Edinburgh. HMSO.

- 991 Noble, S.R., Hyslop, E.K. & Highton, A.J. 1996. High-precision U—Pb monazite geochronology of the c. 806 Ma
992 Grampian Shear Zone and the implications for the evolution of the Central Highlands of Scotland. *Journal*
993 *of the Geological Society, London*, **153**, 511-514.
- 994 Nordgulen, O., Bickford, M. E., Nissen, A. L., & Wortman, G. L. (1993). U-Pb zircon ages from the Bindal Batholith,
995 and the tectonic history of the Helgeland Nappe Complex, Scandinavian Caledonides. *Journal of the*
996 *Geological Society, London*, *150*(4), 771–783. <https://doi.org/10.1144/gsjgs.150.4.0771>
- 997 O’Driscoll, B., Day, J. M. D., Walker, R. J., Daly, J. S., McDonough, W. F., & Piccoli, P. M. (2012). Chemical heterogeneity
998 in the upper mantle recorded by peridotites and chromitites from the Shetland Ophiolite Complex, Scotland.
999 *Earth and Planetary Science Letters*, *333–334*, 226–237. <https://doi.org/10.1016/j.epsl.2012.03.035>
- 1000 Oliver, G. J. H., Chen, F., Buchwaldt, R., & Hegner, E. (2000). Fast tectonometamorphism and exhumation in the type
1001 area of the Barrovian and Buchan zones. *Geology*, *28*(5), 459–462.
- 1002 Pedersen, R. B., & Hertogen, J. (1990). Magmatic evolution of the Karmøy Ophiolite Complex, SW Norway:
1003 relationships between MORB-IAT-boninitic-calc-alkaline and alkaline magmatism. *Contributions to Mineralogy*
1004 *and Petrology*, *104*(3), 277–293. <https://doi.org/10.1007/BF00321485>
- 1005 Pedersen, R. B., & Dunning, G. R. (1997). Evolution of arc crust and relations between contrasting sources: U-Pb
1006 (age), Nd and Sr isotope systematics of the ophiolitic terrain of SW Norway. *Contributions to Mineralogy and*
1007 *Petrology*, *128*(1), 1–15. <https://doi.org/10.1007/s004100050289>
- 1008 Prave, A.R., Strachan, R.A. & Fallick, A.E. 2009. Global C cycle perturbations recorded in marbles: a record of
1009 Neoproterozoic Earth history within the Shetland Islands, Scotland. *Journal of the Geological Society, London*,
1010 *166*, 129-135.
- 1011 Prichard, H. M. (1985). The Shetland ophiolite. In D. G. Gee & B. A. Sturt (Eds.), *The Caledonide Orogen - Scandinavian*
1012 *and Related Areas* (pp. 1173–1184). New York: Wiley.
- 1013 Prichard, H. M., Lord, R. A., & Neary, C. R. (1996). A model to explain the occurrence of platinum- and palladium-rich
1014 ophiolite complexes. *Journal of the Geological Society, London*, *153*, 323–328.
- 1015 Pringle, I. R. (1970). The structural geology of the North Roe area of Shetland. *Geological Journal*, *7*(1), 147–170.
- 1016 Ritchie, J. D., Hitchen, K., & Mitchell, J. G. (1987). The offshore continuation of the Moine Thrust north of Shetland
1017 as deduced from basement isotopic ages. *Scottish Journal of Geology*, *23*(2), 163–173.
1018 <https://doi.org/10.1144/sjg23020163>

- 1019 Roberts, D. (2003). The Scandinavian Caledonides: event chronology, palaeogeographic settings and likely modern
1020 analogues. *Tectonophysics*, 365(1–4), 283–299. [https://doi.org/10.1016/S0040-1951\(03\)00026-X](https://doi.org/10.1016/S0040-1951(03)00026-X)
- 1021 Roberts, D., & Gee, D. G. (1985). An introduction to the structure of the Scandinavian Caledonides. *The Caledonide*
1022 *orogen—Scandinavia and related areas*, 1, 55-68
- 1023 Roberts, D., Nordgulen, Ø., & Melezhik, V. (2007). The Uppermost Allochthon in the Scandinavian Caledonides: From
1024 a Laurentian ancestry through Taconian Orogeny to Scandian crustal growth on Baltica. *Memoir of the*
1025 *Geological Society of America*, 200(18), 357–377. [https://doi.org/10.1130/2007.1200\(18\)](https://doi.org/10.1130/2007.1200(18))
- 1026 Rogers, G., Hyslop, E.K., Strachan, R.A., Paterson, B.A. & Holdsworth, R.E. 1998. The structural setting and U—Pb
1027 geochronology of Knoydartian pegmatites in W. Inverness-shire: evidence for Neoproterozoic
1028 tectonothermal events in the Moine of NW Scotland. *Journal of the Geological Society, London*, 155, 685-
1029 696.
- 1030 Sanders, I.S., Van Calsteren, P.W.C. & Hawkesworth, C.J. 1984. A Grenville Sm—Nd age for the Glenelg eclogite in
1031 northwest Scotland. *Nature*, 312, 439-440, doi: 10.1038/312439a0.
- 1032 Scherer, E. E. S., Cameron, K. L., & Blichert-toft, J. (2000). Lu – Hf garnet geochronology: Closure temperature relative
1033 to the Sm – Nd system and the effects of trace mineral inclusions. *Geochimica et Cosmochimica Acta*, 64(19),
1034 3413–3432.
- 1035 Seranne, M. (1992). Devonian extensional tectonics versus Carboniferous inversion in the northern Orcadian basin.
1036 *Journal of the Geological Society, London*, 149(1), 27–37. <https://doi.org/10.1144/gsjgs.149.1.0027>
- 1037 Skora, S., Baumgartner, L. P., Mahlen, N. J., Johnson, C. M., Pilet, S., & Hellebrand, E. (2006). Diffusion-limited REE
1038 uptake by eclogite garnets and its consequences for Lu–Hf and Sm–Nd geochronology. *Contributions to*
1039 *Mineralogy and Petrology*, 152(6), 703–720. <https://doi.org/10.1007/s00410-006-0128-x>
- 1040 Slagstad, T., Saalman, K., Kirkland, C.L., Høyen, A.B., Storruste, B.K., Coint, N., Pin, C., Marker, M., Bjerkgård, T., Krill,
1041 A., Solli, A., Boyd, R., Larsen, T. & Larsen, R.B. 2020. Late Neoproterozoic through Silurian tectonic evolution of
1042 the Rödingsfället Nappe Complex, orogen-scale correlations and implications for the Scandian suture. This
1043 volume.
- 1044 Smit, M. A., Scherer, E. E., Bröcker, M., & van Roermund, H. L. M. (2010). Timing of eclogite facies metamorphism in
1045 the southernmost Scandinavian Caledonides by Lu-Hf and Sm-Nd geochronology. *Contributions to Mineralogy*
1046 *and Petrology*, 159(4), 521–539. <https://doi.org/10.1007/s00410-009-0440-3>

- 1047 Smit, M. A., Scherer, E. E., & Mezger, K. (2013). Lu-Hf and Sm-Nd garnet geochronology: Chronometric closure and
1048 implications for dating petrological processes. *Earth and Planetary Science Letters*, 381, 222–233.
1049 <https://doi.org/10.1016/j.epsl.2013.08.046>
- 1050 Soper, N. J., Strachan, R. A., Holdsworth, R. E., Gayer, R. A., & Greiling, R. O. (1992). Sinistral transpression and the
1051 Silurian closure of Iapetus. *Journal of the Geological Society, London*, 149, 871–880.
- 1052 Spray, J. G. (1988). Thrust-related metamorphism beneath the Shetland Islands oceanic fragment, northeast
1053 Scotland. *Canadian Journal of Earth Sciences*, 25, 1760–1776.
- 1054 Spray, J. G., & Dunning, G. R. (1991). A U/Pb age for the Shetland Islands oceanic fragment, Scottish Caledonides:
1055 evidence from anatectic plagiogranites in “layer 3” shear zones. *Geological Magazine*, 128, 667–671.
- 1056 Strachan, R. A., Prave, A. R., Kirkland, C. L., & Storey, C. D. (2013). U-Pb detrital zircon geochronology of the Dalradian
1057 Supergroup, Shetland Islands, Scotland: implications for regional correlations and Neoproterozoic-Palaeozoic
1058 basin development. *Journal of the Geological Society, London*. <https://doi.org/10.1144/jgs2013-057>
- 1059 Strachan, R.A., Johnson, T.E., Kirkland, C.L, Kinny, P.D. & Kusky, T. 2020a. A Baltic heritage in Scotland: basement
1060 terrane transfer during the Grenville Orogeny. *Geology*, in press.
1061
- 1062 Strachan, R.A., Alsop, G.I., Ramezani, J., Fraser, R.E., Burns, I.M. & Holdsworth, R.E. 2020b. Patterns of Silurian
1063 deformation and magmatism related to ductile thrusting in the northern Scottish Caledonides. *Journal of the*
1064 *Geological Society of London*, in press.
- 1065 Tanner, P. W. G. (2014). A kinematic model for the Grampian Orogeny, Scotland. *Geological Society, London, Special*
1066 *Publications*, 390(1), 467–511. <https://doi.org/10.1144/SP390.23>
- 1067 Tanner, P.W.G. & Evans, J.A. 2003. Late Precambrian U-Pb titanite age for peak regional metamorphism and
1068 deformation (Knoydartian orogeny) in the western Moine, Scotland. *Journal of the Geological Society,*
1069 *London*, 160, 555-564.
- 1070 Thirlwall, M. F., & Anczkiewicz, R. (2004). Multidynamic isotope ratio analysis using MC-ICP-MS and the causes of
1071 secular drift in Hf, Nd and Pb isotope ratios. *International Journal of Mass Spectrometry*, 235(1), 59–81.
1072 <https://doi.org/10.1016/j.ijms.2004.04.002>

- 1073 Vance, D., Strachan, R.A. & Jones, K.A. 1998. Extensional versus compressional settings for metamorphism: garnet
1074 chronometry and pressure-temperature-time histories in the Moine Supergroup, northwest Scotland.
1075 *Geology*, **26**, 927-930.
- 1076 Vermeesch, P. (2018). IsoplotR: A free and open toolbox for geochronology. *Geoscience Frontiers*, *9*(5), 1479–1493.
1077 <https://doi.org/10.1016/j.gsf.2018.04.001>
- 1078 Viete, D. R., Oliver, G. J. H., Fraser, G. L., Forster, M. A., & Lister, G. S. (2013). Timing and heat sources for the
1079 Barrovian metamorphism, Scotland. *Lithos*, *177*, 148–163. <https://doi.org/10.1016/j.lithos.2013.06.009>
- 1080 Walker, S., Thirlwall, M. F., Strachan, R. A., & Bird, A. F. (2016). Evidence from Rb-Sr mineral ages for multiple
1081 orogenic events in the Caledonides of Shetland, Scotland. *Journal of the Geological Society, London*, *173*, 489–
1082 503. <https://doi.org/10.1144/jgs2015-034>
- 1083 Watts, L. M., Holdsworth, R. E., Sleight, J. A., Strachan, R. A., & Smith, S. A. F. (2007). The movement history and fault
1084 rock evolution of a reactivated crustal-scale strike-slip fault: The Walls Boundary Fault Zone, Shetland. *Journal*
1085 *of the Geological Society, London*, *164*(5), 1037–1058. <https://doi.org/10.1144/0016-76492006-156>
- 1086 Wilson, R. W., Holdsworth, R. E., Wild, L. E., McCaffrey, K. J. W., England, R. W., Imber, J., & Strachan, R. A. (2010).
1087 Basement-influenced rifting and basin development: A reappraisal of post-Caledonian faulting patterns from
1088 the North Coast Transfer Zone, Scotland. *Geological Society Special Publication*, *335*, 795–826.
1089 <https://doi.org/10.1144/SP335.32>
- 1090 Yakymchuk, C., Brown, M., Clark, C., Korhonen, F.J., Piccoli, P.M., Siddoway, C.S., Taylor, R.J.M. and Vervoort, J.D.,
1091 (2015). Decoding polyphase migmatites using geochronology and phase equilibria modelling. *Journal of*
1092 *Metamorphic Geology*, *33*(2), 203-230.
- 1093 Yoshinobu, A. S., Barnes, C. G., Nordgulen, Ø., Prestvik, T., Fanning, M., & Pedersen, R. B. (2002). Ordovician
1094 magmatism, deformation, and exhumation in the Caledonides of central Norway: An orphan of the Taconic
1095 orogeny? *Geology*, *30*(10), 883–886. [https://doi.org/10.1130/0091-7613\(2002\)030<0883:OMDAEI>2.0.CO;2](https://doi.org/10.1130/0091-7613(2002)030<0883:OMDAEI>2.0.CO;2)

1096 **Figure and table captions**

- 1097
- 1098 **Fig. 1.** (A) Regional context of Shetland in its pre-Mesozoic rifting setting (modified from Bird et
1099 al. 2013) NHT – Northern Highland Terrane; MTZ = Moine Thrust Zone; GGF – Great Glen Fault;

1100 SUF – Southern Uplands Fault; HBF – Highland Boundary Fault; IS – Iapetus Suture; CB – Clew Bay
1101 (B) Geological map of Shetland including sample locations.

1102

1103 **Fig. 2.** Speculative, sketch cross-section of the orogenic wedge in the Shetland region following
1104 west-directed ophiolite obduction and Grampian I folding and ductile thrusting, and showing the
1105 east-facing recumbent fold which developed east of the Walls Boundary Fault (the Shetland
1106 ‘mega-monocline’ of Flinn 2007). Late (Mesozoic?) east-side-down displacement on the Bluemull
1107 Sound Fault resulted in the present juxtaposition of lower, west-dipping (east Yell) and upper,
1108 east-dipping (Unst) fold limbs. The kinematic significance of this fold is uncertain, one possibility
1109 is that it resulted from backthrusting, perhaps in combination with underthrusting/tectonic
1110 wedging of a basement block. SVG, Sand Voe Group; YSG, Yell Sound Group; WMC, Walls
1111 Metamorphic Complex; WBF, Walls Boundary fault; A, Archaean; WG, Westing Group; SG, Scatsta
1112 Group, WNG, Whiteness Group; CHG, Clif Hills Group; BSF, Bluemull Sound Fault.

1113

1114 **Fig. 3.** Example of the relationship of colour, trace-element characteristics, and age of garnets.
1115 This is sample SW13-27 from the Hillswick Peninsula in western Mainland Shetland.

1116

1117 **Fig. 4.** Geological map of Shetland with sample locations and garnet ages placed in geographical
1118 setting.

1119

1120 **Fig. 5.** Thin section photographs of samples (A) SW15-12, (B) SW15-07, (C) SW12-16, and (D)
1121 SW12-15 along with LA-ICPMS traverse data for those samples. Note that the LA-ICPMS traverses
1122 were not determined on the minerals shown in this figure, and that they are representative of
1123 the garnets in each sample. Mineral abbreviations from Kretz (1983).

1124

1125 **Fig. 6.** Graphical representation of Caledonian Lu-Hf and Sm-Nd garnet ages determined in this
1126 study, along with those from other modern geochronological studies from metamorphic
1127 lithologies in Shetland. 1 = Walker et al. 2016; 2 = Crowley & Strachan 2015; 3 = Cutts et al. 2011;
1128 4 = Jahn et al. 2017.

1129

1130 **Table 1.** Locations, lithologies, geological significance, and mineral assemblages of the dated
1131 samples. WG – Wilgi Geos group; WKSZ – Wester Keolka Shear Zone; SVG – Sand Voe Group; EG
1132 – Eastern Gneisses; WMS – Walls Metamorphic Series; BFL – Burra Firth Lineament; YSG – Yell
1133 Sound Group; EMS – East Mainland Succession. Mineral abbreviations from Kretz (1983).

1134

1135 **Table 2.** Lu-Hf and Sm-Nd data and ages. Samples marked with * are not considered robust and
1136 are not discussed in the text. Ages in italics are multi-point isochrons. Samples marked with §
1137 were analysed at the Institute of Geological Sciences, Polish Academy of Sciences, Kraków. All
1138 uncertainties are stated at 2σ . Mineral abbreviations from Kretz (1983).

1139

1140

Table 1.

Sample	Location	Grid Ref	Lithology	Geological significance	Mineral assemblage
West of the WBF					
SW15-12	North Roe	HU 34860 91768	WG Garnet amphibolite	Metamorphism west of the WKSZ	Amph+Ep+Qtz+Grt+Bt+Opaque
AB08-11	Fethaland	HU 37230 93435	SVG Benigarth Pelite	Eastern Gneiss basement	Qtz+Wm+Bt+Chl+Grt+Opaque+Tur
AB08-12	Fethaland	HU 37388 93234	Amphibolite	Eastern Gneiss basement	Qtz+Pl+Mc+Amph+Grt+Ttn+Zo+Rt+Wm+Ap+Chl
AB08-13	Burra Voe	HU 37410 89054	SVG Pelitic schist	Moine-equivalent	Grt+Wm+Qtz+Chl+Ttn+Chd
SW13-8	Burra Voe	HU 37340 89159	EG Amphibolite	Interleaved basement inlier	Amph+Qtz+Grt+Wm+Bt+Czt+Ap+Zrc+Rt
SW13-27	Hillswick	HU 2795 7723	EG Pelite	Metamorphism in the Eastern Gneisses	Amph+Qtz+Plag+Wm+Rt+Grt+Chl+Zrc+Bt
SW15-5	Queyfirth	HU 354 829	Amphibolite	Metamorphism in the Eastern Gneisses	Amph+Qtz+Ep+Bt+Grt+Ap+Zrc+Ttn
SW15-01	Shaabers Head	HU 27817 59096	WMS pelite	Metamorphism in the WMS	Qtz+Kspar+Pl+Wm+Bt+Chl+Grt+Opaque
SW15-3	Neeans	HU 27249 59112	WMS Granite gneiss	Metamorphism in the WMS	Qtz+Kspar+Wm+Chl+Bt+Ep+Zrc+Grt+Rt
SW15-6	West Burrafirth	HU 24896 56918	WMS amphibolite	Metamorphism in the WMS	Qtz+Kspar+Pl+Bt+Chl+Grt+Zrc+Opaque+Amph+Ap+Rt
East of the WBF					
Mainland					
SW12-7	East Burrafirth	HU 3695 5080	Semi-pelitic gneiss	Metamorphism in Central Mainland	Qtz+Pl+Wm+Ep+Grt
AB08-18	Lunna Ness	HU 51842 74106	Valayre Gneiss amphibolite	Metamorphism of the Valayre Gneiss	Qtz+Amph+Pl+Grt+Opaque+Ttn
Yell					
AB08-4	Sands of Breckon	HP 52751 05341	YSG paragneiss	Migmatisation of the YSG	Qtz+Pl+Wm+Bt+Grt+Opaque+Ap+Zrc+Ttn+Rt+Chl
AB08-6	Migga Ness	HP 53974 05230	Basement amphibolite	Basement metamorphism	Qtz+Cpx+Amph+Pl+Ttn+Opaques
AB08-8	Kirkrabister	HU 54004 9501	Amphibolite	Prograde metamorphism in the YSG	Grt+Amph+Pl+Qtz+Opaques+Zrc
SW12-20	North Sandwick	HP 5501 9696	Pelite	Prograde metamorphism in the YSG	Qtz+Kspar+Bt+Wm+Chl+Grt+Ky+Zrc+Gr+Rt
Unst					
AB08-14	Westing Group	HP 56784 07120	Gneiss	Metamorphism in the	Qtz+Pl+Wm+Bt+Grt+Ky+Stau+Opaque+Zrc+Sill

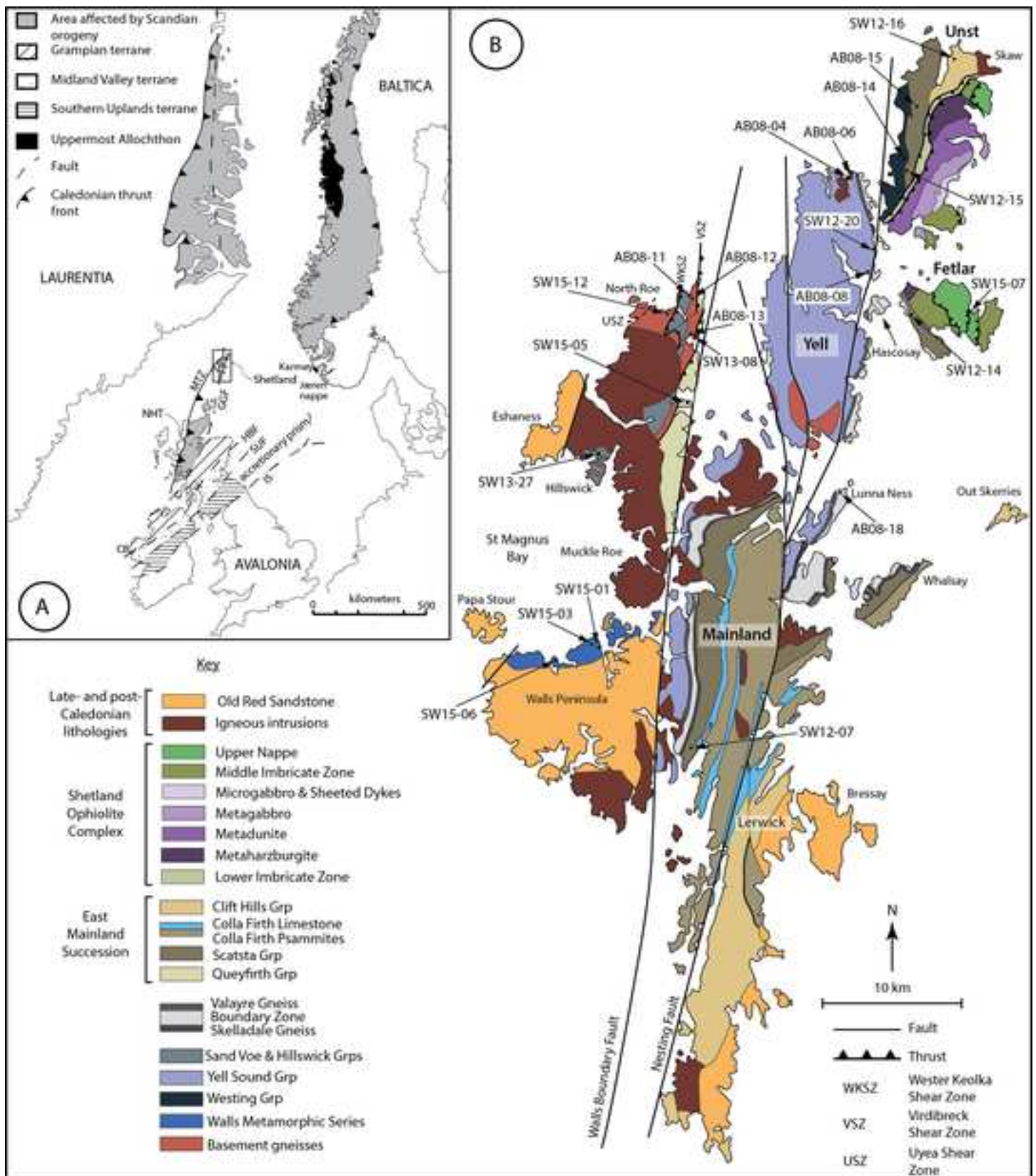
AB08-15	Burrafirth	HP 58766 11098	Valla Field Pelite	Westing Group Metamorphism W of the BFL	Qtz+Plag+Wm+Bt+St+Ky+And+Sil+Grt+Chd+Chl+Zrc+Opaque
SW12-15	W. of Watlee	HP 5814 0548	Valla Field Pelite	Metamorphism W of the BFL	Qtz+Wm+Opaque+Staur+Ky+Chd+Chl
SW12-16	Saxa Vord	HP 6315 1652	Saxa Vord Pelite	Metamorphism E of the BFL	Wm+Chd+Grt+Chl+Opaque+Staur+Qtz
Fetlar					
SW12-14	Hamars Ness	HU 5789 9287	EMS migmatitic schist	High grade met in ophiolite footwall	Qtz+Pl+Kspar+Wm+Bt+Grt+Chl+Opaque+Zrc+Rt
SW15-7	Virva	HU 64449 92009	Metabasite	Metamorphic sole of the ophiolite	Cpx+Pg+Grt+Ttn+Cal+Chl

Table 2.

Sample fraction	Lu ppm	Hf ppm	¹⁷⁶ Lu/ ¹⁷⁶ Hf	¹⁷⁶ Hf/ ¹⁷⁷ Hf	2se	¹⁷⁶ Hf/ ¹⁷⁷ Hf ₀	Age (Ma)	Sm ppm	Nd ppm	¹⁴⁷ Sm/ ¹⁴⁴ Nd	¹⁴³ Nd/ ¹⁴⁴ Nd	2se		
<i>West of the WBF</i>														
SW15-12 wr tt	0.3094	0.5355	0.08164	0.283025	0.000018									
SW15-12 grt	3.047	0.4930	0.8746	0.289363	0.000025	0.282353±20	426.9±2.5							
AB08-11 wr §	0.5813	2.970	0.02766	0.282493	0.000006	X		3.639	15.01	0.1466	0.511967	0.000007	X	
AB08-11 wr fl *	0.5858	5.245	0.01578	0.282437	0.000008	0.282305±8	446.5±1.3							
AB08-11 grt red §	4.845	1.464	0.4680	0.286221	0.000008	N=3	MSWD=0.17	1.508	6.772	0.1346	0.512001	0.000007	X	
AB08-11 grt ora §	7.408	1.214	0.8634	0.289522	0.000012			0.7020	2.859	0.1484	0.512039	0.000008	X	
AB08-12 wr tt	0.7099	1.042	0.09629	0.283517	0.000009	X		4.727	17.41	0.1641	0.512440	0.000006	X	
AB08-12 wr fl*	0.7184	5.163	0.01966	0.282576	0.000009	0.282399±10	479.6±1.2							
AB08-12 grt 1	2.728	0.3711	1.0405	0.291758	0.000016		MSWD=1.4	0.2947	1.1172	0.1595	0.512432	0.000010	X	
AB08-12 grt 2	0.5118	0.0553	1.3107	0.294164	0.000017			1.711	6.465	0.1600	0.512445	0.000005	X	
AB08-12 amph	0.2014	0.9177	0.03101	0.283157	0.000006	X		4.373	15.88	0.1665	0.512493	0.000006	X	
AB08-13 wr tt	0.4289	2.672	0.02268	0.282402	0.000009	X		4.019	17.87	0.13594	0.511779	0.000009		
AB08-13 wr fl*	0.5228	7.371	0.01002	0.282247	0.000005								470±6	
AB08-13 grt ora	3.742	1.0393	0.5092	0.286517	0.000013	0.282161±5	456.7±2.0	4.563	22.44	0.12291	0.511748	0.000011		
AB08-13 grt pur	1.793	4.548	0.05572	0.282746	0.000006	0.282138±6	582±9*	1.890	2.753	0.4151	0.512643	0.000009	0.511358±14	
SW13-08 wr tt								2.581	13.40	0.11650	0.512453			
SW13-08 wr fl*	0.3684	2.063	0.02523	0.282707	0.000049									
SW13-08 grt ora §	3.547	0.3110	1.616	0.296601	0.000014	0.282487±50	466.3±2.2							
SW13-08 grt red §	3.839	0.8053	0.6744	0.288297	0.000007	0.282490±50	459.7±4.3							
SW15-01 wr tt	0.289	0.2367	0.171	0.283595	0.000051									
SW15-01 wr fl*	0.3193	7.092	0.00636	0.281940	0.000005									
SW15-01 grt Ora	4.922	2.804	0.2481	0.284269	0.000018	0.281879±5	514.1±4.4							
SW15-01 grt Pink	4.548	2.015	0.3190	0.284919	0.000010	0.281879±5	508.5±2.5							
SW15-03 wr tt	0.4036	0.2782	0.2051	0.283871	0.000032	X		4.459	21.74	0.12396	0.511810	0.000010		
SW15-03 wr fl*	0.4145	8.122	0.00721	0.282111	0.000006									
SW15-03 grt ora	8.736	15.90	0.07765	0.283022	0.000008	0.282018±6	689±8*	1.906	2.924	0.3942	0.512903	0.000013	0.511309±16	617±9

SW15-03 grt red	6.798	2.897	0.3318	0.285068	0.000011	0.282045±6	486.3±2.5	1.641	1.900	0.5224	0.513045	0.000016	0.511426±14	473.2±7.2
SW15-05 wr tt §	0.620	0.9137	0.095	0.283284	0.000016									
SW15-05 wr fl	0.6415	4.702	0.01928	0.282252	0.000011									
SW15-05 grt §	2.024	0.2324	1.234	0.293400	0.000074	0.282426±15	474.3±3.5							
SW15-06 wr tt §	0.7507	5.186	0.02045	0.282405	0.000012			9.273	47.46	0.11810	0.511925	0.000009		
SW15-06 wr fl	0.8067	9.529	0.01196	0.282299	0.000008	N=3	MSWD=0.93							
SW15-06 grt ora	7.218	3.668	0.2782	0.285407	0.000010	0.282162±7	621.9±3.1	0.9478	0.5520	1.0386	0.514710	0.000020	0.511568±10	461.9±3.7
SW15-06 grt pink	15.36	4.207	0.5164	0.288039	0.000010	0.282163±8	606.4±2.9	2.019	1.0078	1.2121	0.515388	0.000034	0.511551±11	483.3±4.9
						N=3	MSWD=1.7							
SW13-27 wr tt §	0.2744	0.2816	0.1377	0.283187	0.000019			2.311	9.605	0.1455	0.511470	0.000006		
SW13-27 wr fl	0.2913	3.527	0.01167	0.282078	0.000011									
SW13-27 grt ora §	3.298	0.9347	0.4990	0.286266	0.000013	0.281978±11	458.8±2.3	0.8421	1.867	0.2727	0.511868	0.000010	0.511015±17	478±14
SW13-27 grt red §	3.935	1.123	0.4955	0.286183	0.000012	0.281979±11	453.0±2.3	1.0058	2.649	0.2295	0.511748	0.000010	0.510988±24	505±21
East of the WBF														
Mainland														
SW12-07 wr tt	0.2093	0.6808	0.04344	0.282583	0.000020	X		0.8049	2.405	0.2023	0.512022	0.000018		
SW12-07 wr fl	0.2255	1.234	0.02583	0.282394	0.000044									
SW12-07 grt	47.06	1.438	4.659	0.323966	0.000013	0.282162±44	479.0±1.5	4.830	0.5261	5.572	0.528577	0.000026	0.511398±18	470.7±1.0
AB08-18 wr tt	0.7555	1.968	0.05427	0.283061	0.000007									
AB08-18 grt ora	3.053	0.6278	0.6881	0.288637	0.000023	0.282584±8	469.6±2.5							
AB08-18 grt red	3.417	1.1798	0.4096	0.286050	0.000009	0.282605±8	449.2±2.3							
AB08-18 grt pink	2.886	1.1863	0.3439	0.285436	0.000017	0.282616±9	437.9±3.7							
Yell														
AB08-04 wr tt								4.388	21.83	0.1215	0.511842	0.000009		
AB08-04 grt								2.487	0.5463	2.757	0.519908	0.000021	0.511470±9	467.2±1.4
AB08-06 wr tt	0.7905	0.4009	0.2789	0.287950	0.000037	X		3.256	9.754	0.2019	0.512864	0.000012		
AB08-06 wr fl	0.7745	1.467	0.07464	0.284861	0.000030									
AB08-06 grt	4.518	0.1193	6.735	0.416718	0.000080	0.283383±32	1051.2±3.2	2.849	1.743	0.9891	0.517320	0.000013	0.511721±16	863.1±3.6
AB08-08 wr tt	0.8507	0.4315	0.2787	0.285073	0.000023	0.282707±16	453.6±5.1	2.521	4.735	0.3218	0.512924	0.000015	0.511916±19	478.1±2.3

SW12-14 wr fl	0.4198	7.100	0.00835	0.281933	0.000008									
SW12-14 grt 1	7.801	1.983	0.5564	0.286919	0.000007			0.9167	1.1249	0.4927	0.512731	0.000011	0.511264±8	453.7±3.8
SW12-14 grt 2	7.860	1.985	0.5601	0.286935	0.000008			0.8715	0.8987	0.5863	0.513002	0.000014	N=3	MSWD=0.64
SW12-14 grt pink §	7.742	1.978	0.5536	0.286885	0.000008			0.9355	1.4208	0.3980	0.512473	0.000011	0.511251±8	472±10
SW12-14 grt ora §	8.545	2.243	0.5388	0.286731	0.000016	0.281857±4	484.5 ± 1.4	0.9835	1.5489	0.3839	0.512444	0.000010	N=3	MSWD=3.8
							MSWD=1.6							
SW15-07 cpx §	0.0879	0.7649	0.01624	0.282801	0.000034									
SW15-07 grt core §	3.840	0.3192	1.705	0.298404	0.000078									
SW15-07 amph §	0.1685	1.145	0.02079	0.282912	0.000044									
SW15-07 grt rim §	2.592	0.3688	0.9950	0.291772	0.000096	N=4, MSWD 4.1	491.4±5.5							

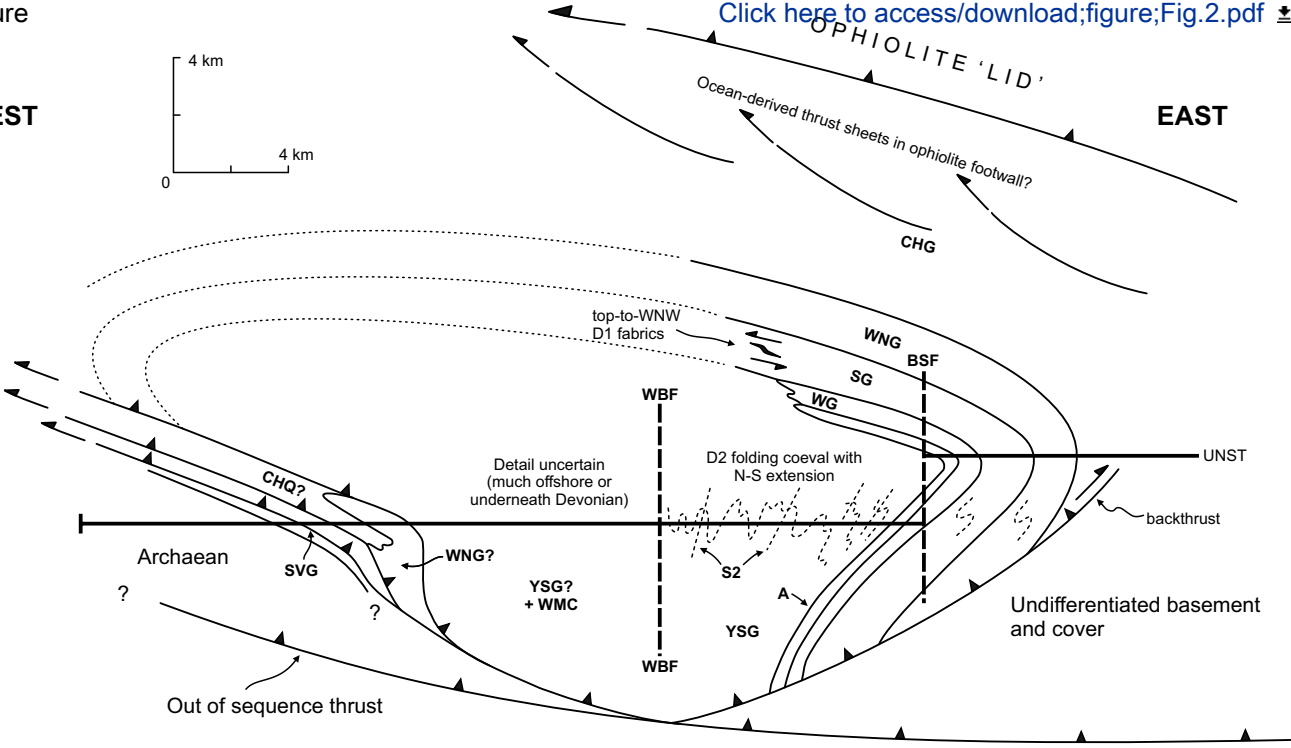
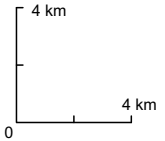


figure

[Click here to access/download;figure;Fig.2.pdf](#)

WEST

EAST



Archaean

?

Out of sequence thrust

SVG

WNG?

YSG?
+ WMC

WBF

WBF

YSG

A

S2

Detail uncertain
(much offshore or
underneath Devonian)

D2 folding coeval with
N-S extension

WNG

SG

WG

BSF

UNST

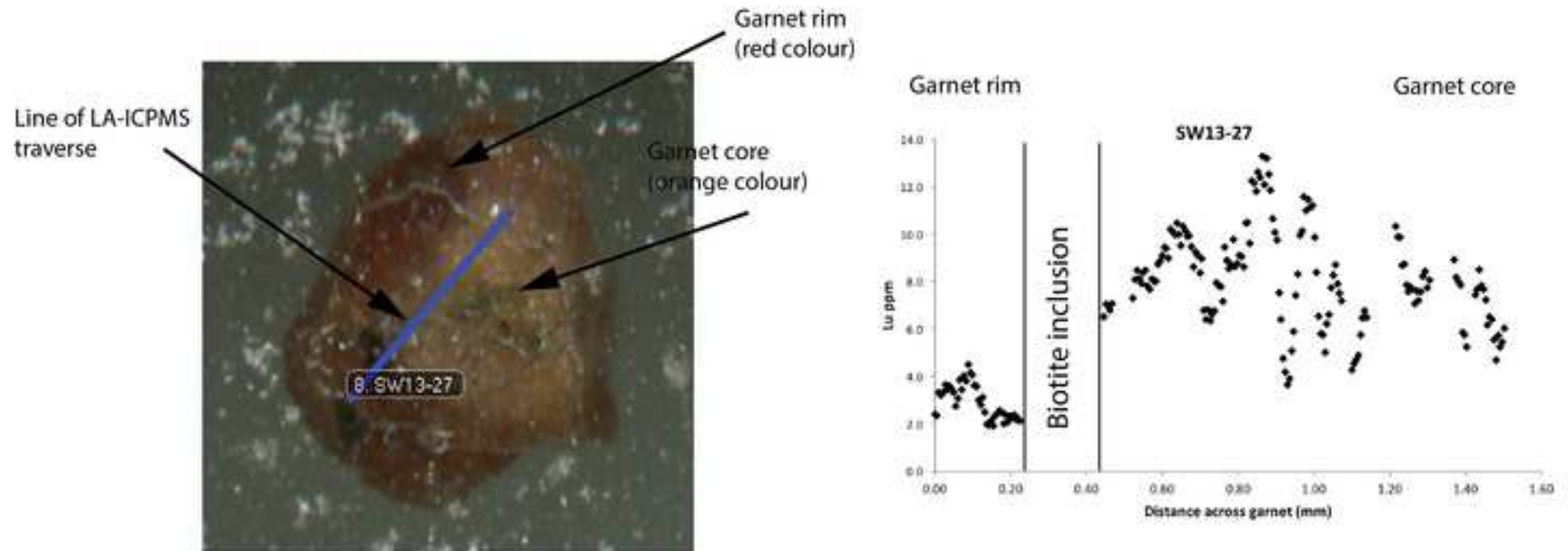
backthrust

Undifferentiated basement
and cover

OPHIOLITE 'LID'

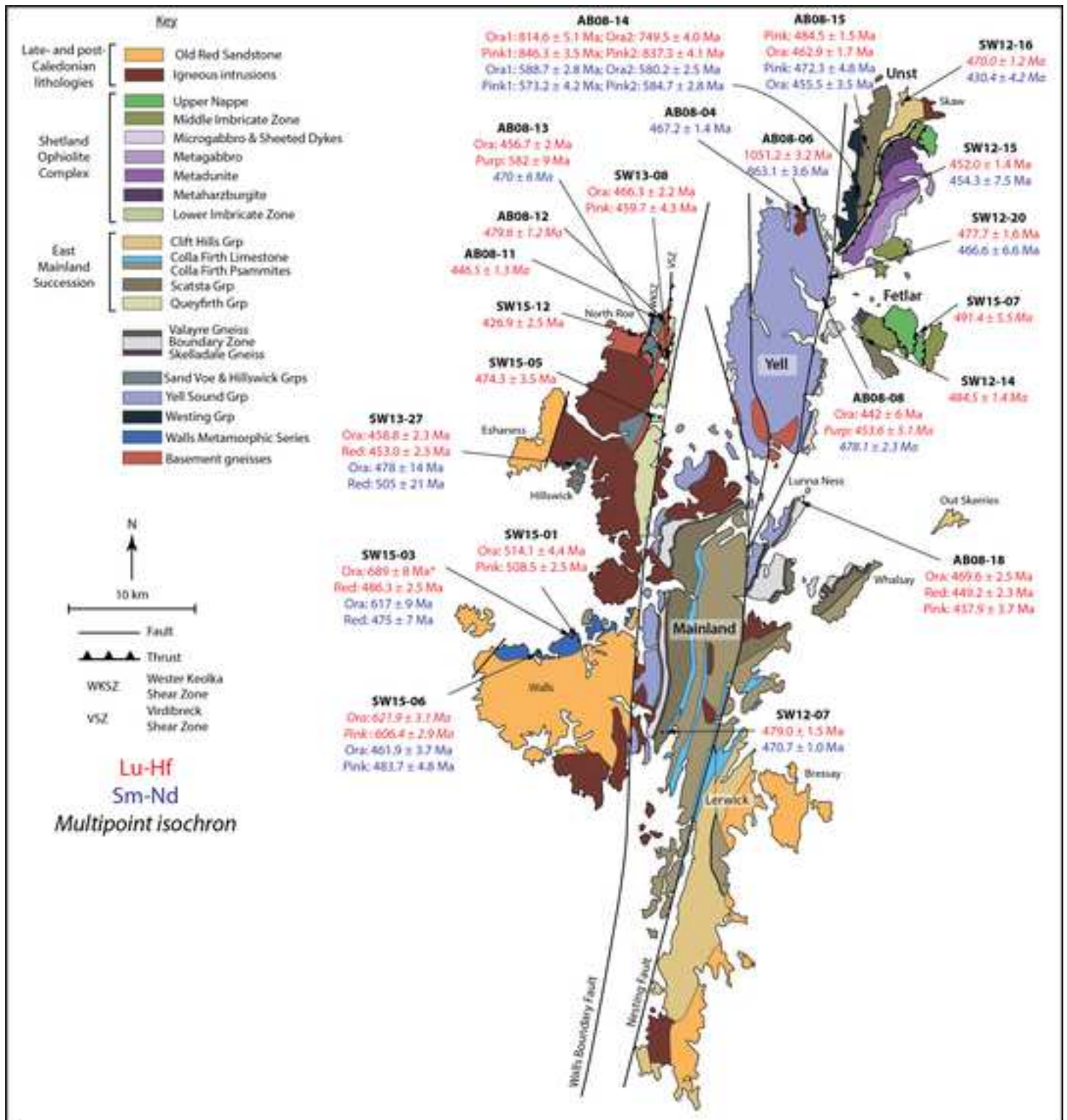
Ocean-derived thrust sheets in ophiolite footwall?

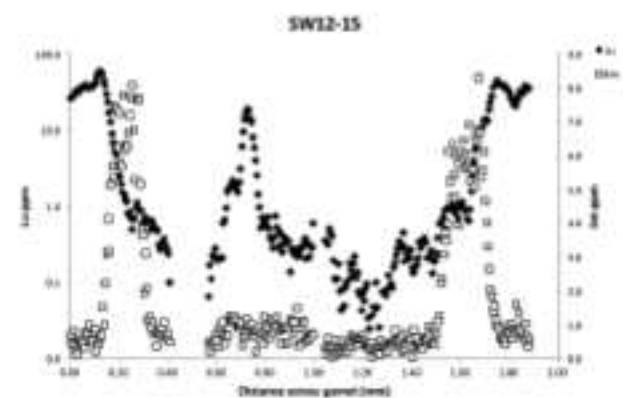
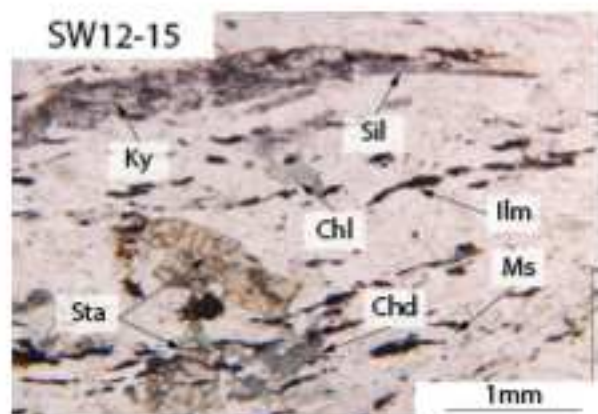
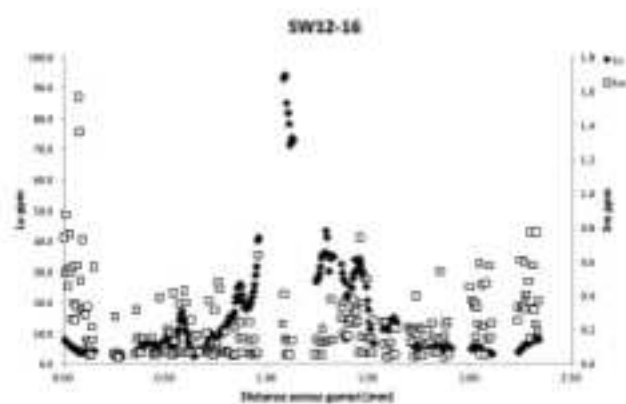
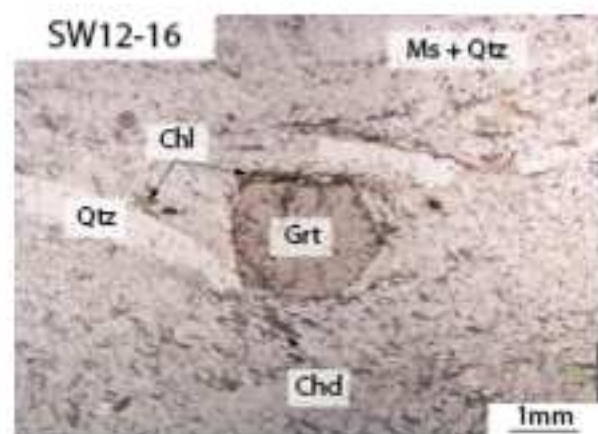
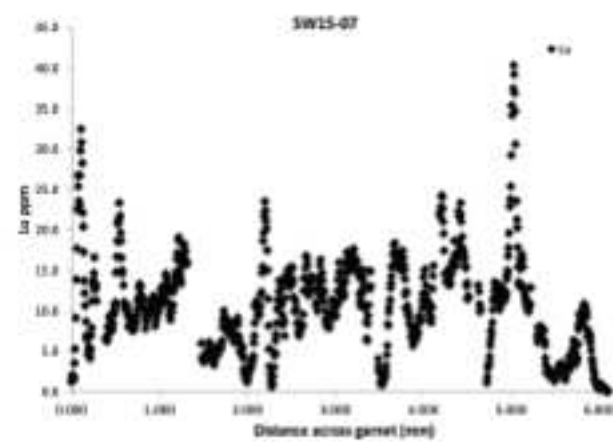
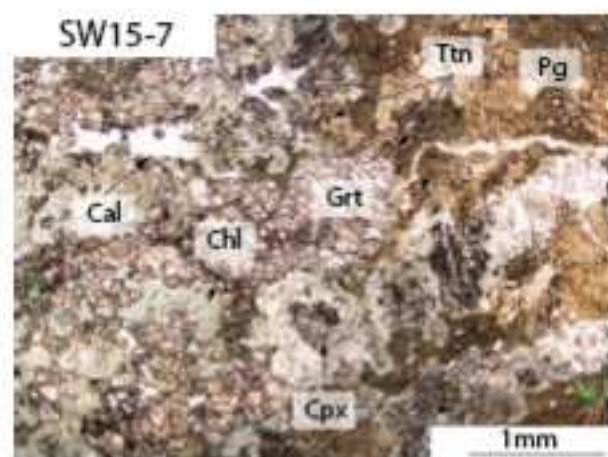
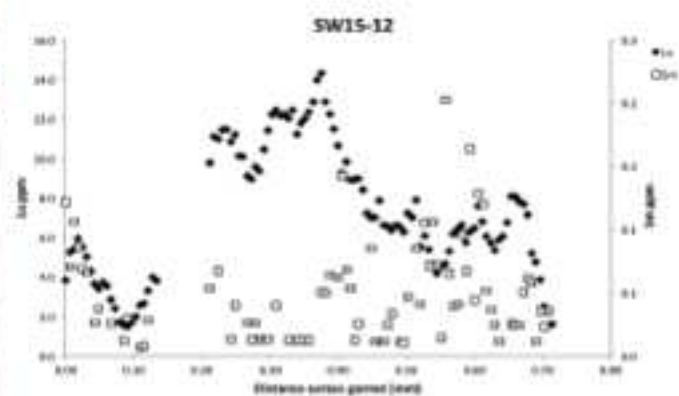
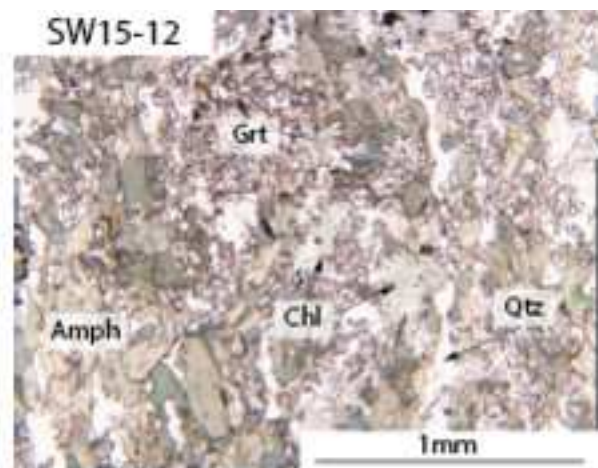
CHG

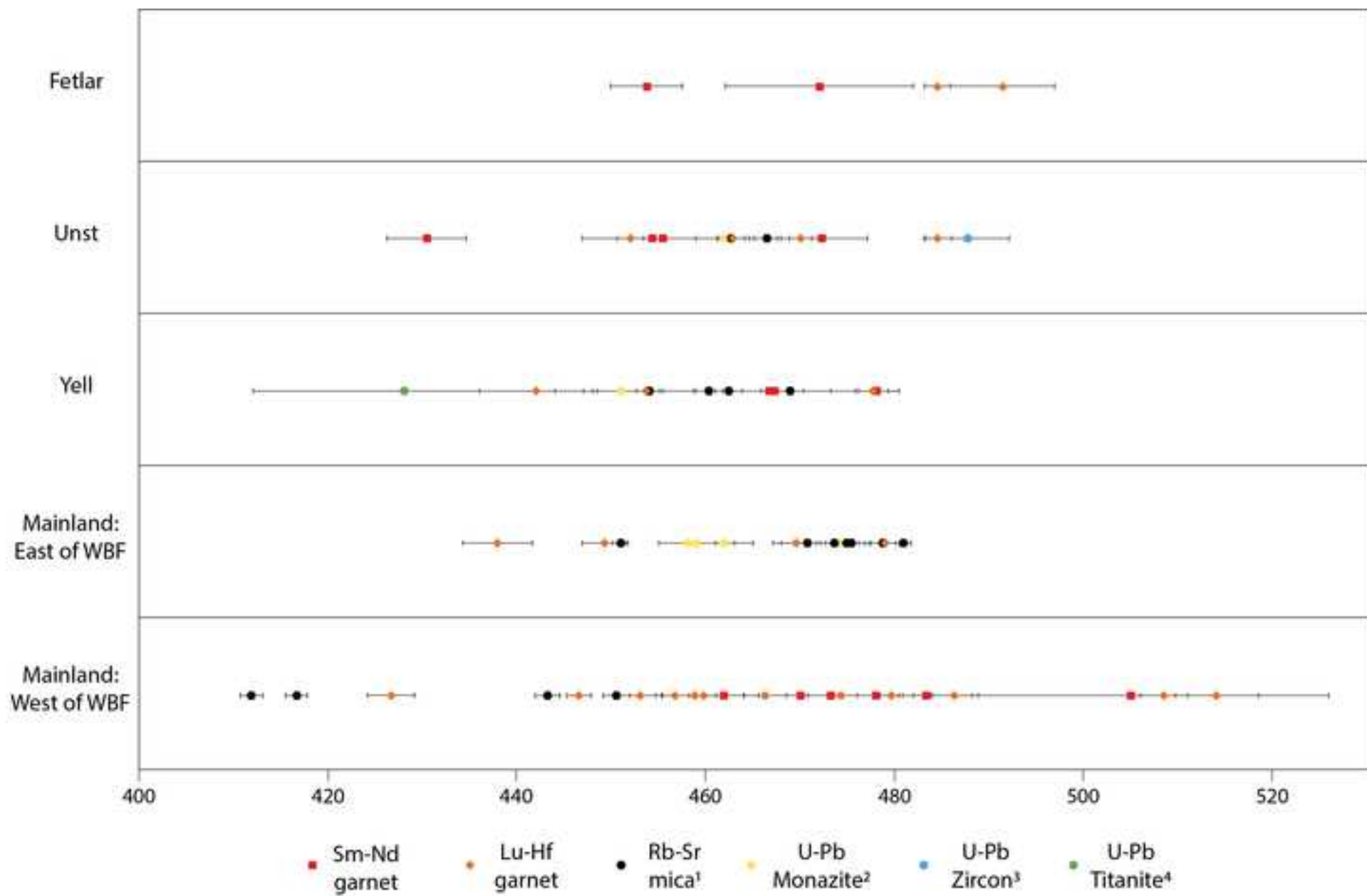


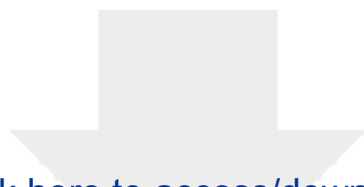
Garnet core (picked as 'orange') Lu-Hf age: 458.8 ± 2.3 Ma

Garnet rim (picked as 'red') Lu-Hf age: 453.0 ± 2.3 Ma

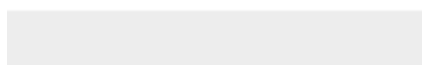
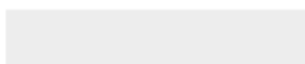








Click here to access/download
supplementary material (not datasets)
SuppData1_XRF.xlsx





Click here to access/download
supplementary material (not datasets)
SuppData2_LA-ICPMS.xlsx

